

Deterministic Neural Networks with Appropriate Inductive Biases Capture Epistemic and Aleatoric Uncertainty

Jishnu Mukhoti^{*1,2}Andreas Kirsch^{*1}Joost van Amersfoort¹Philip H.S. Torr²Yarin Gal¹^{*}Joint first authors¹OATML, University of Oxford²Torr Vision Group, University of Oxford

Abstract

We show that a single softmax neural net with minimal changes can beat the uncertainty predictions of Deep Ensembles and other more complex single-forward-pass uncertainty approaches. Softmax neural nets cannot capture epistemic uncertainty reliably because for OoD points they extrapolate arbitrarily and suffer from feature collapse. This results in arbitrary softmax entropies for OoD points which can have high entropy, low, or anything in between. We study why, and show that with the right inductive biases, softmax neural nets trained with maximum likelihood reliably capture epistemic uncertainty through the feature-space density. This density is obtained using Gaussian Discriminant Analysis, but it cannot disentangle uncertainties. We show that it is necessary to combine this density with the softmax entropy to disentangle aleatoric and epistemic uncertainty—crucial e.g. for active learning. We examine the quality of epistemic uncertainty on active learning and OoD detection, where we obtain SOTA ~ 0.98 AUROC on CIFAR-10 vs SVHN.

1 INTRODUCTION

Two types of uncertainty are often of interest: *epistemic uncertainty*, which is inherent to the model, caused by a lack of training data, and hence reducible with more data, and *aleatoric uncertainty*, caused e.g. by inherent noise and ambiguity in data, and hence irreducible [Der Kiureghian and Ditlevsen, 2009, Kendall and Gal, 2017]. Disentangling these two uncertainties is critical for active learning [Gal et al., 2017] and out-of-distribution (OoD) detection [Hendrycks and Gimpel, 2016]. This matters in particular for noisy and ambiguous datasets as might be found in safety-critical applications like autonomous driving [Huang and Chen, 2020] and medical diagnosis [Esteva et al., 2017,

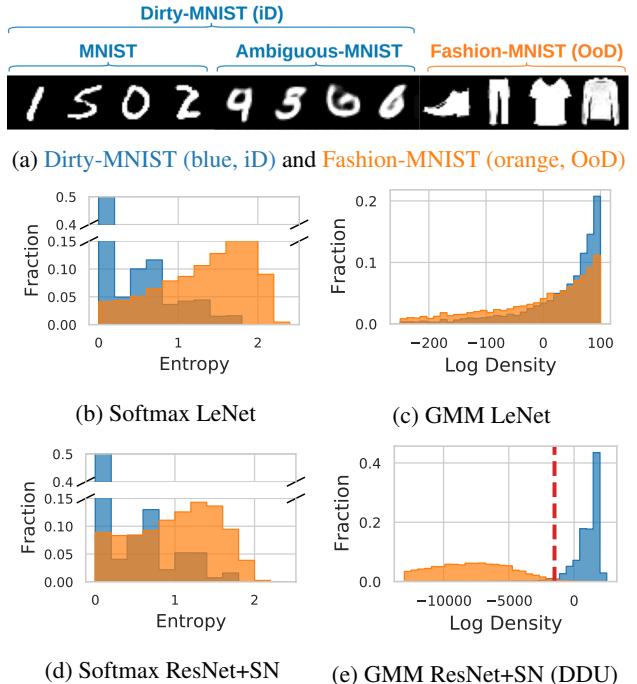


Figure 1: *OoD separation of networks without and with appropriate inductive biases (LeNet vs ResNet+SN resp.), using softmax entropy (left) and feature-space density (GMM, right). All trained on Dirty-MNIST as in-distribution (iD) and evaluated on Fashion-MNIST as OoD, see (a). (b) & (d): Softmax entropy has arbitrary values for OoD, indistinguishable from iD, thus cannot detect OoD. (c) & (e): Without appropriate inductive bias, LeNet feature density suffers from feature collapse and cannot capture epistemic uncertainty or detect OoD either, whereas ResNet+SN can.*

Filos et al., 2019].

Most well-known methods of uncertainty quantification in deep learning [Blundell et al., 2015, Gal and Ghahramani, 2016, Lakshminarayanan et al., 2017, Wen et al., 2019, Dusenberry et al., 2020] require multiple forward passes at test time which can represent a significant computational overhead. Amongst these, Deep Ensembles [Lakshminaray-

anan et al., 2017] generally have performed best in uncertainty prediction [Ovadia et al., 2019]. Ensembling neural networks, however, poses an even more significant memory and compute overhead at training and test time. It is often computationally prohibitive to implement these methods, which hinders adoption in real-life applications. Consequently, there has been an increased interest in uncertainty quantification using deterministic neural networks which quantify uncertainty in a single forward pass and therefore have a smaller memory footprint and lower latency.

Two recent works in single-forward-pass uncertainty, DUQ [van Amersfoort et al., 2020] and SNGP [Liu et al., 2020a], propose distance-aware output layers, in the form of RBF or Gaussian processes (GP); and regularisers or inductive biases on the encoder, in the form of a Jacobian penalty [Gulrajani et al., 2017] or spectral normalisation [Miyato et al., 2018]. These methods perform well and are competitive with Deep Ensembles on common benchmarks. However, they either do not differentiate between epistemic and aleatoric uncertainty, or, due to the specialised RBF and GP output layers, require specialised training regimes and additional hyper-parameters, which further hinders adoption.

In this paper, we introduce *Deep Deterministic Uncertainty (DDU)* and show that by enforcing smoothness and sensitivity (using a bi-Lipschitz constraint) [van Amersfoort et al., 2020, Rosca et al., 2020] on the feature-space through inductive biases, e.g. spectral normalisation [Miyato et al., 2018] and residual connections [He et al., 2016], a single softmax neural network trained with maximum likelihood can reliably capture epistemic uncertainty through its feature-space density, with no adaptations required for its training procedure. While sensitivity prevents feature collapse, smoothness ensures that the feature-space density can be obtained using a distance-based density estimator. Given a pre-trained softmax neural network with such inductive biases, we use Gaussian Discriminant Analysis (GDA) which fits a Gaussian Mixture Model (GMM) with one Gaussian per class on the feature space of the pre-trained network [Murphy, 2012]. Without sensitivity and smoothness, the feature-space density alone might not separate in-distribution (iD) from OoD data (illustrated in fig. 1(c)), possibly explaining the shortcomings of previous approaches which model feature-space density [Lee et al., 2018b, Postels et al., 2020].

Finally, we find that by combining information from both the feature-space density and the softmax entropy, we can effectively disentangle epistemic and aleatoric uncertainty, and we show that this is necessary as a single output layer cannot generally be optimal for both.

To illustrate the above, in fig. 1 we train a LeNet [LeCun et al., 1998] and a second model with our inductive biases—ResNet-18 [He et al., 2016] with spectral normalisation (ResNet+SN)—on *Dirty-MNIST*, a modified version of

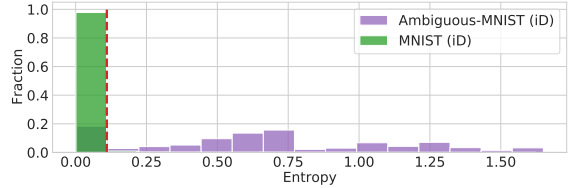


Figure 2: *Softmax entropy histogram of a ResNet+SN trained on Dirty-MNIST separating MNIST vs Ambiguous-MNIST, both iD.* Aleatoric uncertainty is captured correctly.

MNIST [LeCun et al., 1998] with additional ambiguous digits (Ambiguous-MNIST). Refer to Appendix A for details on how this dataset was generated. *Ambiguous-MNIST* contains samples with multiple plausible labels and thus, higher aleatoric uncertainty (see fig. 1(a)). With such ambiguous data having various levels of aleatoric uncertainty, Dirty-MNIST is more representative of real-world datasets, as compared to well-known curated datasets, like MNIST and CIFAR-10, commonly used for benchmarking in machine learning [Filos et al., 2019, Krizhevsky et al., 2009]. This poses a challenge for conventional OoD detection methods, which often confound aleatoric and epistemic uncertainty.

From fig. 1(b) and (d), we note that the entropy of a deterministic model is unable to distinguish between iD (Dirty-MNIST) and OoD (Fashion-MNIST [Xiao et al., 2017]) samples as the entropy for the latter heavily overlaps with the entropy for Ambiguous-MNIST samples. However, the feature-space density of the ResNet+SN model in fig. 1(e) captures epistemic uncertainty reliably and is able to distinguish iD from OoD samples. The same cannot be said for LeNet in fig. 1(c), whose density is unable to separate OoD from iD samples. This demonstrates the importance of the inductive bias to ensure sensitivity and smoothness of the feature space as we argue below. Finally, using insights from fig. 1(e) and fig. 2, we construct a method to separate aleatoric from epistemic uncertainty: Samples with low feature density have high epistemic uncertainty whereas those with both high feature density and high softmax entropy have large aleatoric uncertainty (note the high softmax entropy for Ambiguous MNIST samples in fig. 2).

The paper is organised as follows. First, in section 3 we **i**) prove we cannot infer epistemic uncertainty from a deterministic softmax model’s softmax entropy (and in fact, this is tied to the very reason why deep ensemble uncertainty works), hence we must resort to alternatives such as feature-space density; **ii**) argue that feature collapse leads to a failure in capturing epistemic uncertainty from a deterministic softmax model’s feature-space density, and enforcing smoothness and sensitivity on the feature space alleviates this problem; **iii**) argue that we need both softmax entropy and feature density to disentangle epistemic uncertainty from aleatoric uncertainty; and **iv**) prove that we must use separate output layers for aleatoric and epistemic uncertainty because a single generative classifier cannot generally

be optimal for both. Second, in section 4 we detail how to implement our approach, DDU, with no change to training procedure and minimal changes to softmax models. Finally, through extensive experiments on relevant tasks like OoD detection and active learning, we demonstrate that with a single deterministic model with appropriate inductive biases we are able to outperform Deep Ensemble Uncertainty and other deterministic uncertainty baselines in uncertainty quantification, while maintaining high accuracy.

2 BACKGROUND

In this section, we provide a brief overview of approaches for quantifying uncertainty in deep learning and discuss related work to motivate our approach.

Bayesian Models Neal [2012], MacKay [1992] provide a principled way of measuring uncertainty. Starting with a prior distribution $p(\omega)$ over model parameters ω , they infer a posterior $p(\omega|\mathcal{D})$, given the training data \mathcal{D} . The predictive distribution $p(y|x, \mathcal{D})$ for a given input x is computed via marginalisation over the posterior: $p(y|x, \mathcal{D}) = \mathbb{E}_{\omega \sim p(\omega|\mathcal{D})}[p(y|x, \omega)]$. As mentioned in Gal [2016], Smith and Gal [2018], the predictive entropy $\mathbb{H}[Y|x, \mathcal{D}]$ of $p(y|x, \mathcal{D})$ upper-bounds the epistemic uncertainty, given as the mutual information $\mathbb{I}[Y; \omega|x, \mathcal{D}]$ (*information gain*) between parameters ω and output y , following the equation:

$$\underbrace{\mathbb{H}[Y|x, \mathcal{D}]}_{\text{predictive}} = \underbrace{\mathbb{I}[Y; \omega|x, \mathcal{D}]}_{\text{epistemic}} + \underbrace{\mathbb{E}_{p(\omega|\mathcal{D})}[\mathbb{H}[Y|x, \omega]]}_{\text{aleatoric (for iD x)}}. \quad (1)$$

The intractability of exact Bayesian inference in deep learning has led to the development of methods for approximate inference [Hinton and Van Camp, 1993, Hernández-Lobato and Adams, 2015, Blundell et al., 2015, Gal and Ghahramani, 2016]. In practice, however, these methods are either unable to scale well to large datasets and model architectures, suffer from low uncertainty quality, or require expensive Monte-Carlo sampling.

Deep Ensembles Lakshminarayanan et al. [2017] train an ensemble of neural networks and average their predictions as the model output, which is a simple and effective way to estimate uncertainty. Although incurring a high computational overhead at training and test time, deep ensembles, along with recent extensions [Wen et al., 2019, Dusenberry et al., 2020] form the current state-of-the-art in uncertainty quantification in deep learning. It is interesting to note that ensembling can also be seen as performing Bayesian model averaging [Wilson and Izmailov, 2020], as each ensemble member, producing a softmax output $p(y|x, \omega)$, can be considered to be drawn after training from some distribution $p(\omega|\mathcal{D})$ over the model parameters ω , which is induced by the weight initialization and stochastic optimization over the dataset. As a result, eq. (1) can also be applied to deep ensembles in order to disentangle epistemic from predictive uncertainty.

In practice, both mutual information $\mathbb{I}[Y; \omega|x, \mathcal{D}]$ and predictive entropy $\mathbb{H}[Y|x, \mathcal{D}]$, are used in the literature to detect OoD samples. As seen in eq. (1), predictive entropy can be high for both ambiguous samples, with high aleatoric uncertainty, and OoD samples, with high epistemic uncertainty. Hence, it is only an effective measure for OoD detection when used with curated datasets that do not contain ambiguous samples, as shown in fig. 1.

Deterministic Models produce a softmax distribution $p(y|x, \omega)$ and use either the maximum softmax probability: $\max_c p(y = c|x, \omega)$ as a measure of confidence or the softmax entropy $\mathbb{H}[Y|x, \omega]$ as uncertainty. It is well-known that these measures are often overconfident on OoD data and even on misclassified iD samples [Hendrycks and Gimbel, 2016, Guo et al., 2017]. Popular approaches to tackle this problem include pre-processing of inputs and post-hoc calibration methods [Liang et al., 2018, Guo et al., 2017], alternative objective functions [Lee et al., 2018a, DeVries and Taylor, 2018], and exposure to outliers [Hendrycks et al., 2018]. However, these methods suffer from several shortcomings including failure to perform under distribution shift [Ovadia et al., 2019], requiring significant changes to the training setup and assuming the availability of OoD samples during training. In the next section, we demonstrate that the softmax entropy is inherently inappropriate to capture epistemic uncertainty.

Feature-Space Distances and Density offer a different approach for estimating uncertainty in deterministic models [Lee et al., 2018b, van Amersfoort et al., 2020, Liu et al., 2020b,a, Postels et al., 2020]. This approach assumes that epistemic uncertainty increases outside the training distribution in feature space. Postels et al. [2020] propose using the density of the feature space in different layers as measure of epistemic uncertainty and the entropy of the inferred predictive distribution given the density for each class as a measure of aleatoric uncertainty. They find that deeper layers provide better aleatoric uncertainty while shallower layers provide better epistemic uncertainty. None of these methods, however, are able beat the current state-of-the-art (i.e., deep ensembles) in uncertainty quantification, potentially for the reasons discussed next.

Feature Collapse is introduced in van Amersfoort et al. [2020] as a reason as to why density estimation in the feature space may fail to capture epistemic uncertainty out of the box: feature extractors learn invariances which cause them to map OoD samples to iD regions in feature space. To fix this issue, a feature extractor f_θ , with parameters θ , can be subjected to a bi-Lipschitz constraint as follows:

$$K_1 \|x_1 - x_2\|_I \leq \|f_\theta(x_1) - f_\theta(x_2)\|_F \leq K_2 \|x_1 - x_2\|_I, \quad (2)$$

for all inputs, x_1 and x_2 , where $\|\cdot\|_I$ and $\|\cdot\|_F$ denote metrics in the input and feature space respectively, and K_1 and K_2 denote the lower and upper Lipschitz constants [Liu et al., 2020a]. As discussed in van Amersfoort et al. [2020], the

lower Lipschitz bound ensures *sensitivity* to distances in the input space, thereby ensuring sensitivity to OoD samples. At the same time, the upper Lipschitz bound ensures *smoothness* in the features, preventing them from becoming too sensitive to input variations, which, otherwise, can lead to poor generalisation and a loss of robustness [Hess et al., 2020, Rosca et al., 2020]. In practice, popular ways of ensuring the bi-Lipschitz condition include: **i)** gradient penalty, by applying a two-sided penalty to the L2 norm of the Jacobian [Gulrajani et al., 2017], and **ii)** spectral normalisation [Miyato et al., 2018] in models with residual connections, like ResNets [He et al., 2016].

Feature-space approaches are not as different from softmax outputs for uncertainty quantification as it might seem because **softmax layers are implicit GMMs** [Murphy, 2012]. A softmax layer $p(y|z) = \text{Softmax}(Wz + b)$ is equivalent to the predictive probabilities $q(y|z)$ of a generative classifier $q(y, z)$ in feature space obtained using *Linear Discriminant Analysis (LDA)* [Murphy, 2012, Lee et al., 2018b, Hess et al., 2020]. While in GDA each class’s component has its own covariance matrix, in LDA the class-conditional probabilities $q(z|y)$ use a single multi-variate Gaussian per class, with covariance matrix $\Sigma \in \mathbb{R}^{|z| \times |z|}$ shared amongst the classes: $q(z|y = c) \sim \mathcal{N}(z; \mu_c, \Sigma)$. Given a class prior $q(y)$, the predictive probabilities $q(y|z)$ can be computed using Bayes’ theorem, while marginalising over the class-conditional probabilities $q(z) = \sum_c q(z|y = c)$ yields the density $q(z)$. This unifying perspective allows us to treat softmax layers like other generative classifiers. For one, we recover a feature-space density from a standard softmax layer similar to Liu et al. [2020b], and we see that more general generative classifiers, like GDA, can fit the feature representation of a softmax model after training at least as well as the model’s softmax layer itself.

3 UNCERTAINTY IN DETERMINISTIC SOFTMAX MODELS

In this section, we motivate DDU step by step. Additional formalisations and proofs for all statements in this section are provided in the appendix F.

Softmax entropy cannot capture epistemic uncertainty because deep ensembles can. As mentioned in section 2, eq. (1) can be used with deep ensembles, as each ensemble member can be considered a sample from *some* distribution $p(\omega | \mathcal{D})$ over model parameters $\omega \subset \Omega$ (e.g. a uniform distribution over K ensemble members $\omega_1, \dots, \omega_K$). In fact, the mutual information $\mathbb{I}[Y; \omega | x, \mathcal{D}]$ isolates epistemic from aleatoric uncertainty for deep ensembles as well, whereas the predictive entropy $\mathbb{H}[Y | x, \mathcal{D}]$ (often used with deep ensembles) measures predictive uncertainty (it will be high whenever either epistemic or aleatoric uncertainties are high). Further, the mechanism underlying deep ensemble uncertainty that pushes epistemic uncertainty to

be high on OoD data is function disagreement between different ensemble components, i.e. ‘arbitrary extrapolations’ of the softmax models composing the ensemble (leading the ‘aleatoric’ term in eq. (1) to vanish [Smith and Gal, 2018]). From this and eq. (1), we can draw the following conclusion:

Proposition 3.1. *Let x_1 and x_2 be points such that x_1 has higher epistemic uncertainty than x_2 under the ensemble: $\mathbb{I}[Y_1; \omega | x_1, \mathcal{D}] > \mathbb{I}[Y_2; \omega | x_2, \mathcal{D}]$. Further assume both have equal predictive entropies $\mathbb{H}[Y_1 | x_1, \mathcal{D}] = \mathbb{H}[Y_2 | x_2, \mathcal{D}]$. Then, there exist sets of ensemble members Ω_1, Ω_2 with $p(\Omega_1 | \mathcal{D}) > 0$ and $p(\Omega_2 | \mathcal{D}) > 0$, such that for all $\omega_1 \in \Omega_1$ and $\omega_2 \in \Omega_2$ the softmax entropy of x_1 is **lower** than the softmax entropy of x_2 : $\mathbb{H}[Y_1 | x_1, \omega_1] < \mathbb{H}[Y_2 | x_2, \omega_2]$.*

The above proposition shows that if a sample is assigned higher epistemic uncertainty (in the form of mutual information) by a deep ensemble, it will necessarily be assigned lower softmax entropy by at least one of the ensemble’s members. As a result, *the empirical observation that the mutual information of an ensemble quantifies epistemic uncertainty implies that the softmax entropy of a deterministic model cannot*. This claim is further supported by fig. 1(b) and (d) (and appendix E) where we observe the softmax entropy for OoD samples to be spread out (having values which can be high, low or anywhere in between). The failure of softmax entropy to capture epistemic uncertainty motivates us to study feature-space density as an alternative.

Capturing epistemic uncertainty in feature space requires sensitivity and smoothness. As discussed in Section 2, feature extractors without sensitivity and smoothness constraints on their feature space can suffer from feature collapse: they might map OoD samples to iD regions of the feature space. van Amersfoort et al. [2020] argue that sensitivity and smoothness are necessary for capturing epistemic uncertainty and show this empirically. At the same time, Liu et al. [2020a] show that a bi-Lipschitz constraint ensures both smoothness and sensitivity, and find that spectral normalisation together with residual connections are sufficient for the feature extractor to become bi-Lipschitz, thereby allowing a model to learn a feature space amenable to density estimation which captures epistemic uncertainty. This motivates our choice to use spectral normalisation and residual connections for DDU.

Disentangling epistemic and aleatoric uncertainty, in our setting, is surprisingly not trivial as we show in the following observation.

Observation 3.2. *Neither the softmax entropy of a deterministic model, nor its feature density alone, even with sensitivity and smoothness, can be used to disentangle epistemic from aleatoric uncertainty.*

A feature-density estimator fit on iD data cannot generally estimate aleatoric uncertainty. An iD sample ought to

have a high density regardless of whether it is ambiguous (with high aleatoric uncertainty) or not, as is the case with Dirty-MNIST (see Section 1). Further, as we prove next, the softmax probability induced by the feature-density estimator will generally not be well-calibrated as there is an objective mismatch. On the other hand, softmax entropy, cannot capture epistemic uncertainty. As seen in Figure 1, it can be high, low or anywhere in between for OoD samples, and cannot be distinguished from ambiguous iD samples.

This was overlooked in previous research on uncertainty quantification for deterministic models [Lee et al., 2018b, Liu et al., 2020a, van Amersfoort et al., 2020, He et al., 2016] as they do not consider ambiguous samples which can be found in many real world applications.

From this, we conclude that we can use softmax entropy to capture aleatoric uncertainty for iD samples and feature-space density to capture epistemic uncertainty. This combination allows us to disentangle aleatoric and epistemic uncertainty in deterministic models.

Capturing aleatoric and epistemic uncertainty requires multiple generative classifiers because a single generative classifier, whether implicit as a softmax layer or explicit using LDA or GDA, cannot be optimal for both feature-space density and predictive distribution estimation:

Proposition 3.3. *For an input x , let $z = f_\theta(x)$ denote its feature representation in a feature extractor f_θ with parameters θ . Then the following hold:*

1. *A discriminative classifier $p(y|z)$, e.g. a softmax layer, is well-calibrated in its predictions when it maximises the conditional log-likelihood $\log p(y|z)$;*
2. *A feature-space density estimator $q(z)$ is optimal when it maximises the marginalised log-likelihood $\log q(z)$;*
3. *A hidden-latent model $q(y,z)$ cannot generally maximise both objectives, conditional log-likelihood and marginalised log-likelihood, at the same time. In the specific instance that it does maximise both, the resulting model must be a GDA (but the opposite does not hold).*

Note that if the two objectives coincide, then the resulting model must be a GDA. But the opposite is not true—given a GDA, the two objectives might not coincide. Consequently, we use both a discriminative classifier and a feature-density estimator on a model that was trained using conditional log-likelihood (cross-entropy objective): we fit a density estimator on the feature representations of the training data to capture epistemic uncertainty, and use the softmax entropy to capture aleatoric uncertainty.

4 ALGORITHM

We use the insights developed in the sections above, and propose a deterministic neural network with appropriate inductive biases to satisfy our conditions. Additionally we

show how to disentangle its uncertainties, which enable us to outperform Deep Ensemble Uncertainty on standard OoD detection benchmarks.

Ensuring sensitivity & smoothness: We encourage the model to learn a feature representation such that OoD samples are not mapped near iD feature representations. In this work, we use networks that lower bound the Lipschitz constant by using residual connections and upper bound the Lipschitz constant using spectral normalisation. This method is preferred over using Jacobian gradient penalty because it is significantly faster and more reliable [Liu et al., 2020a]. Additionally, we make minor changes to the model architecture to improve uncertainty quality without sacrificing accuracy, which we detail in appendix B.

Disentangling epistemic & aleatoric uncertainty: DDU is trained using a softmax output on a maximum likelihood (cross-entropy) objective. In order to quantify epistemic uncertainty, a feature-space density model is fitted after training. For this, DDU uses a GDA $q(y,z)$, with a single mixture component per class. We fit each class component of the GDA by computing the empirical mean and covariance, per class, of the feature vectors $z = f_\theta(x)$, which are the outputs of the last convolutional layer of the model computed on the respective training samples x (*we stress that we do not require OoD data to fit these*). This requires just a single pass through the training set given a trained model. At test time, we compute the epistemic uncertainty by evaluating the marginal likelihood of the feature representation under our density $q(z) = \sum_c q(z|y=c)$. To quantify aleatoric uncertainty for in-distribution samples, we use the entropy $H[Y|x, \theta]$ of the softmax distribution $p(y|x, \theta)$. Note that the softmax distribution thus obtained, can be further calibrated using temperature scaling [Guo et al., 2017].

Based on the insights in Section 3, we disentangle aleatoric and epistemic uncertainty in DDU using the following steps:

1. For a given input sample, a high feature-space density indicates low epistemic uncertainty, i.e. the sample is iD, and we can trust the aleatoric uncertainty estimated by the softmax entropy of the model. It can either be unambiguous (low softmax entropy/aleatoric uncertainty) or ambiguous (high softmax entropy/aleatoric uncertainty).
2. A low feature-space density and thus high epistemic uncertainty means that the sample is OoD, and we cannot trust the aleatoric uncertainty estimated by the softmax entropy of the model as it can take any arbitrary value.

5 RELATED WORK

Among approaches that model feature density, Lee et al. [2018b] use Mahalanobis distances to quantify uncertainty by fitting a class-wise Gaussian distribution on the feature space of a pre-trained softmax model. However, they do not constrain the pre-trained feature extractor. As seen in fig. 1(c), the feature density can fail to identify OoD samples

if the model is unable to map OoD feature representations far away from iD ones. Winkens et al. [2020] use contrastive training to improve the feature extractor before estimating the feature-space density. Our method is separate from these works as we restrict ourselves to the supervised setting and show that the inductive biases (bi-Lipschitz) proposed in van Amersfoort et al. [2020], Liu et al. [2020a] is a sufficient condition for the feature-space density to reliably capture epistemic uncertainty. At the same time, our method differs from van Amersfoort et al. [2020], Liu et al. [2020a] by alleviating the need for changes in the training setup as we fit the GMM on the feature space after training. Note that Liu et al. [2020a] also use the softmax entropy of a deterministic network with inductive biases (bi-Lipschitz) as a baseline for comparison and show it to underperform compared to SNGP. In section 3, we provide a detailed explanation as to why their baseline fails.

Postels et al. [2020] propose a density based estimation of aleatoric and epistemic uncertainty in deep models. Note that similar to Lee et al. [2018b], they do not pose any constraints on the feature extractor, which, as we have observed, can lead to feature collapse (see Figure 1(c)). Hence, they report worse epistemic uncertainty in deeper layers. Also, they do not consider the objective mismatch that arises when trying to use the same generative classifier for both epistemic and aleatoric uncertainty. Likewise, Liu et al. [2020b] use the implicit GMM of the softmax layer to compute an un-normalized density for OoD detection without taking into account the objective mismatch (see proposition 3.3).

6 EXPERIMENTS

We show that DDU can disentangle epistemic and aleatoric uncertainty: we evaluate DDU on the quality of epistemic uncertainty estimation in active learning [Cohn et al., 1996] using both clean and ambiguous versions of MNIST. Lastly, we perform OoD detection by training on CIFAR-10 and quantifying how well we can distinguish it from SVHN and CIFAR-100. This is a standard benchmark on which we set new state-of-the-art performance.

6.1 DISENTANGLING EPISTEMIC AND ALEATORIC UNCERTAINTY

In section 1, we motivated the formulation of DDU with the help of a toy example which shows that a single regularised softmax model with a proper inductive bias can reliably capture epistemic uncertainty via its feature-space density and aleatoric uncertainty via its softmax entropy. In this section, we further elaborate on these observations.

Dirty-MNIST & Ambiguous-MNIST: The epistemic uncertainty of a model is expected to be high on OoD data. Aleatoric uncertainty is expected to be high for ambiguous iD samples, such as those that plausibly belong to multiple

| Dataset pair | Model | Epistemic Uncertainty/OoD Detection | AUROC |
|--------------------|--------------------|-------------------------------------|---------------|
| MNIST vs A-MNIST | ResNet-18+SN (DDU) | Softmax Entropy | 0.8965 |
| | ResNet-18+SN | Softmax Entropy | 0.8444 |
| | LeNet | Feature Density | 0.8127 |
| D-MNIST vs F-MNIST | ResNet-18+SN (DDU) | Feature Density | 0.9982 |

Table 1: *AUROC for separating MNIST vs Ambiguous-MNIST (A-MNIST) and Dirty-MNIST (D-MNIST) vs Fashion-MNIST (F-MNIST)*. MNIST vs A-MNIST requires separating clean from ambiguous samples, thereby aleatoric uncertainty. D-MNIST vs F-MNIST requires detecting OoD samples, thereby epistemic uncertainty.

classes or contain observation noise. These are natural characteristics of many real-world datasets, but many “machine-learning-ready” datasets have been overly cleaned to remove such sources of noise. In order to recreate these conditions, we use MNIST [LeCun et al., 1998] as an in-distribution dataset of unambiguous samples, Ambiguous-MNIST as an in-distribution dataset of ambiguous samples and Fashion-MNIST [Xiao et al., 2017] as an OoD dataset. Figure 1(a) shows example elements of these datasets, and Appendix A details how these datasets were constructed. We train a LeNet [LeCun et al., 1998] and a ResNet-18 [He et al., 2016] with spectral normalisation (SN) on Dirty-MNIST (a mix of Ambiguous- and standard MNIST). The training setup is detailed in appendix C.1.

Observations: In table 1, the AUROC scores for separating **i**) MNIST from Ambiguous-MNIST (an application of aleatoric uncertainty estimation) and **ii**) Dirty-MNIST from Fashion-MNIST (an application of epistemic uncertainty estimation) are depicted.

Our baseline model trained with softmax and using entropy as the uncertainty metric captures aleatoric uncertainty well, as expected. DDU obtains an AUROC close to 0.9, indicating a good separation between MNIST and Ambiguous-MNIST (also evident from fig. 2).

However, the AUROC for Dirty-MNIST vs Fashion-MNIST shows that the softmax model that uses entropy as epistemic uncertainty performs poorly when distinguishing these two datasets, lending credence to the claim that softmax entropy does not capture epistemic uncertainty. This is emphasised in fig. 1(b) and 1(d), which show a strong overlap between the softmax entropy of OoD and ambiguous iD samples. We also see that using the feature-space density of LeNet as epistemic uncertainty performs even worse, highlighting why we need a sensitive feature extractor *and* feature density. Just using softmax entropy does not perform well at all. However, combining it with a GMM (obtaining DDU) and using its feature density leads to performance far better (with AUROC of 0.99) than the alternatives in the ablation study in table 1. This result is also depicted by the near perfect separation in the uncertainty density plot in fig. 1(e).

Summary: The entropy of a softmax model can be used to estimate aleatoric uncertainty, even without restrictions on the model, but it *cannot* be used to estimate epistemic uncer-

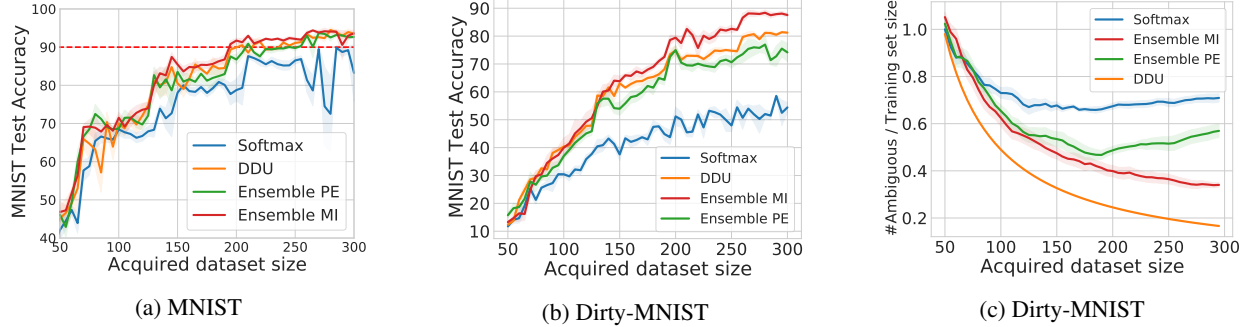


Figure 3: *Active Learning* showing test accuracy vs acquired training set size with MNIST (a) and Dirty-MNIST (b) pool sets; (c): fraction of ambiguous samples chosen in each acquisition step (shaded area shows standard error over 5 repetitions).

tainty (see section 3). On the other hand, feature-space density can *only* be used to estimate epistemic uncertainty when the feature extractor is sensitive and smooth, as achieved by using a ResNet and spectral normalisation in DDU.

6.2 ACTIVE LEARNING

In this section we further study our uncertainty disentanglement with the application of active learning (AL) [Cohn et al., 1996]. AL aims to train models in a data-efficient manner. The goal is to label as few samples as possible while reaching a satisfactory model accuracy. Additional training samples are iteratively acquired from a large pool of unlabelled data and labelled with the help of an expert. After each acquisition step, the model is retrained on the newly expanded training set. This is repeated until the model achieves a desirable accuracy or when a maximum number of samples have been acquired.

Quickly obtaining a high-accuracy model with AL relies on acquiring the most informative samples during each acquisition step. This can be achieved by selecting points with high epistemic uncertainty [Gal et al., 2017]. On the other hand, points with high aleatoric uncertainty are not informative for the model and acquiring leads to data inefficiency—the opposite of what we aim to achieve with AL. AL therefore makes an excellent application for evaluating the quality of epistemic uncertainty estimation and the ability of models to separate different source of uncertainty. We evaluate DDU on two different setups: **i**) with clean MNIST samples in the pool set, and **ii**) with Dirty-MNIST, having a 1:60 ratio of MNIST to Ambiguous-MNIST samples, in the pool set.

Clean MNIST in the Pool set: In this setup, we use normal MNIST samples in the pool set and compare 3 baselines: **i**) a ResNet-18 with softmax entropy as the acquisition function (samples with the top- k softmax entropies are acquired at each step), **ii**) DDU trained using a ResNet-18 with the feature density as the acquisition function (samples with the bottom- k densities are acquired at each step), and **iii**) a Deep Ensemble of 3 ResNet-18s with the predictive entropy (PE) and mutual information (MI) of the ensemble as the acquisition functions (samples with the top- k predictive entropies or mutual informations are acquired at each step).

We start with an initial training-set size of 20 randomly chosen MNIST points, and in each iteration, acquire 5 new samples. For each acquisition step, we train the models using Adam [Kingma and Ba, 2015] for 100 epochs. We stop the process when the training set size reaches 300.

In fig. 3(a), DDU clearly outperforms the deterministic softmax baseline and is competitive with Deep Ensembles. The softmax baseline reaches 90% test-set accuracy at a training-set size of 270. DDU reaches 90% accuracy at training-set size of 200, whereas Deep Ensemble reaches the same at 210 and 195 training samples with PE and MI as the acquisition functions respectively. Note that DDU is three times faster than a Deep Ensemble, which needs to train three models independently after every acquisition.

Dirty-MNIST in the Pool set: The MNIST samples in the pool set of the previous setup lack ambiguity. However, real-life datasets often contain observation noise and ambiguous samples. What happens when the pool set contains a lot of such noisy samples having high aleatoric uncertainty? In such cases, it becomes important for models to identify unseen and informative samples with high epistemic uncertainty and not with high aleatoric uncertainty.

In order to study this scenario in greater detail, we construct a pool set with samples from Dirty-MNIST (see section 6.1). We significantly increase the proportion of ambiguous samples by using a 1:60 split of MNIST to Ambiguous-MNIST (a total of 1K MNIST and 60K Ambiguous-MNIST samples). With this new pool set, we compare DDU with the deterministic softmax baseline as well as the Deep Ensemble baseline with both PE and MI acquisition functions. We increase the number of labelled samples at start to 50.

In fig. 3(b), the difference in the performance of DDU and the deterministic softmax model is stark. While DDU achieves a test set accuracy of 85% at a pool set size of 265 samples, the accuracy of the softmax baseline peaks at a mere 58%. DDU also performs better than Deep Ensembles with the PE acquisition function. From fig. 3(c), it is clear that both the softmax model and the Deep Ensemble using PE as the acquisition function acquires a significantly larger fraction of ambiguous samples in each acquisition step as compared to DDU and Deep Ensemble with MI acquisition.

| Method | Penalty | Aleatoric Uncertainty | Epistemic Uncertainty | Test Accuracy | Test ECE | AUROC SVHN | AUROC CIFAR100 |
|--|---------|-----------------------|-----------------------|------------------|---------------------------------------|-----------------------------------|------------------------------------|
| Softmax | - | Softmax Entropy | Softmax Entropy | 96.18 \pm 0.07 | 0.0073 \pm 0.0007 | 92.99 \pm 1.8 | 88.08 \pm 0.02 |
| Energy-based [Liu et al., 2020b] | - | Softmax Entropy | Softmax Density | 96.18 \pm 0.07 | 0.0073 \pm 0.0007 | 92.79 \pm 2.03 | 87.7 \pm 0.02 |
| DUQ [van Amersfoort et al., 2020] | JP | Kernel Distance | Kernel Distance | 94.6 \pm 0.16 | 0.0155 \pm 0.0008 | 93.71 \pm 0.61 | 85.92 \pm 0.35 |
| SNGP [Liu et al., 2020a] | SN | Predictive Entropy | Predictive Entropy | 96.04 \pm 0.09 | 0.018 \pm 0.001 | 94.0 \pm 1.3 | 91.13 \pm 0.15 |
| 5-Ensemble [Lakshminarayanan et al., 2017] | - | Predictive Entropy | Predictive Entropy | 96.75 \pm 0.04 | 0.0073 \pm 0.0005 | 97.67 \pm 0.04 | 91.43 \pm 0.07 |
| DDU (ours) | SN | Softmax Entropy | GMM Density | 96.38 \pm 0.04 | 0.0073 \pm 0.0004 | 97.9 \pm 0.22 | 91.77 \pm 0.05 |

Table 2: *OoD detection performance of different baselines trained on CIFAR-10 using a Wide-ResNet-28-10 architecture with SVHN and CIFAR-100 as OoD datasets.* Note: SN stands for Spectral Normalisation, JP stands for Jacobian Penalty.

tion. In fact this difference gets larger as the training set size grows. DDU’s feature density and Deep Ensemble’s MI solely capture epistemic uncertainty and hence, do not get confounded by iD ambiguous samples. This leads to the acquisition of unseen points from the pool set which have high epistemic uncertainty and low aleatoric uncertainty (for context, see fig. 1(e)), thereby leading to better performance.

6.3 CIFAR-10 VS SVHN/CIFAR-100

OoD detection is an application of epistemic uncertainty quantification: we expect OoD data points to have higher epistemic uncertainty than iD data. In this experiment, we compare the performance of DDU in OoD detection compared to current state-of-the-art in the field. We train on CIFAR-10 [Krizhevsky et al., 2009] and use SVHN [Netzer et al., 2011] and CIFAR-100 as OoD datasets for this experiment as these dataset pairs (i.e., CIFAR-10 vs SVHN and CIFAR-10 vs CIFAR-100) are known to be difficult [Nalisnick et al., 2019]. The training setup is described in appendix C.2.

Baselines: We use multiple methods including the current state-of-the-art as baselines, and mention the measure used to quantify both aleatoric and epistemic uncertainty in each baseline in Table 2. The aleatoric component is used for evaluating uncertainty measures on the iD test set whereas the epistemic uncertainty is used for evaluating performance on OoD data. The following are the baselines we use for comparison:

1. *Softmax*: We use the softmax entropy of a deterministic model for both aleatoric and epistemic uncertainty.
2. *Energy-based model* [Liu et al., 2020b]: We use the softmax entropy of a deterministic model as aleatoric uncertainty and the softmax density (using the logsumexp of the logits of the model) as epistemic uncertainty without regularisation to avoid feature collapse.
3. *DUQ* [van Amersfoort et al., 2020] and *SNGP* [Liu et al., 2020a]: We compare with the current state-of-the-art deterministic methods for uncertainty quantification including DUQ and SNGP. For SNGP, we use the entropy of the average of the MC softmax samples as uncertainty. For DUQ, we use the closest kernel distance.
4. *5-Ensemble*: We use an ensemble of 5 networks with the same architecture and compute the predictive entropy of the ensemble as both epistemic and aleatoric uncertainty

and mutual information as epistemic uncertainty.

5. *DDU*: As mentioned before, for DDU, we use the softmax entropy as aleatoric uncertainty and the feature density (GMM density) as epistemic uncertainty.

In addition, we also test different ablations of DDU (see appendix D). The ablations include architectures with and without the proposed inductive biases. We use VGG-16 [Simonyan and Zisserman, 2015] as the architecture without any inductive bias (i.e., no residual connections and no spectral normalisation) and Wide-ResNet-28-10 as the architecture with inductive biases. We also test Wide-ResNet-28-10 without spectral normalisation. We report the results for all these ablations in table 3 in the appendix.

Results and Discussion: In table 2, we present the AUROC scores on CIFAR-10 vs SVHN and CIFAR-10 vs CIFAR-100 along with CIFAR-10 test set accuracy and test set ECE (all post temperature scaling). Firstly, for OoD detection (AUROC metrics), DDU outperforms all other methods including the current state-of-the-art Deep Ensembles as well as DUQ and SNGP on both ‘CIFAR-10 vs SVHN’ and ‘CIFAR-10 vs CIFAR-100’. Furthermore, the superior performance in OoD detection comes without compromising on the single-model test set accuracy which slightly improves on that of other single-model accuracies (note that we do not claim to improve accuracy over Deep Ensemble). Secondly, from table 3 (and figure 1(c)), we note that the feature density of softmax models (VGG-16) without the appropriate inductive biases does not perform nearly as well as compared to the models with inductive biases (Wide-ResNet-28-10). This indicates the importance of having the bi-Lipschitz constraint on the model to obtain smoothness and sensitivity (although unlike the figure where we see explicit feature collapse, the differences in performance in the table could also be attributed to additional differences in model architecture). Similarly, using the softmax density for epistemic uncertainty [Liu et al., 2020b] underperforms DDU as well. Note that the Wide-ResNet-28 model without spectral normalisation (see table 3) does indeed have the inductive bias of residual connections built into the model architecture. This can be a contributing factor towards good performance in general as residual connections make the model sensitive to changes in the input space. Finally, note that DDU is amenable to post-hoc calibration in the form of temperature scaling [Guo et al., 2017], which only affects

the softmax output and does not change the GMM density.

7 CONCLUSION

In this paper, we have shown sufficient conditions for a single deterministic model to reliably capture epistemic uncertainty. With appropriate inductive biases, a neural network with a regular off-the-shelf architecture can quantify epistemic uncertainty through its feature space density. Furthermore, by combining this density with the entropy of the softmax distribution, we can effectively disentangle aleatoric from epistemic uncertainty. This is crucial in applications like active learning, which require a reliable estimate of epistemic uncertainty. Through detailed experiments, we show that our method, Deep Deterministic Uncertainty (DDU), while requiring minimal changes to softmax model architectures and keeping the same training method, can outperform the current state-of-the-art on uncertainty quantification including Deep Ensembles on active learning and OoD detection (CIFAR-10 vs SVHN and CIFAR-10 vs CIFAR-100).

8 ACKNOWLEDGEMENTS

The authors would like to thank the members of OATML in general for their feedback at various stages of the project. JM is fully funded by a research grant from Five. AK is supported by the UK EPSRC CDT in Autonomous Intelligent Machines and Systems (grant reference EP/L015897/1). JvA is grateful for funding by the EPSRC (grant reference EP/N509711/1) and Google-DeepMind. This work was also supported by the Royal Academy of Engineering under the Research Chair and Senior Research Fellowships scheme, EPSRC/MURI grant EP/N019474/1.

References

Charles Blundell, Julien Cornebise, Koray Kavukcuoglu, and Daan Wierstra. Weight uncertainty in neural network. In *International Conference on Machine Learning*, pages 1613–1622. PMLR, 2015.

David A Cohn, Zoubin Ghahramani, and Michael I Jordan. Active learning with statistical models. *Journal of artificial intelligence research*, 4:129–145, 1996.

Thomas M Cover. *Elements of information theory*. John Wiley & Sons, 1999.

Armen Der Kiureghian and Ove Ditlevsen. Aleatory or epistemic? does it matter? *Structural safety*, 31(2):105–112, 2009.

Terrance DeVries and Graham W Taylor. Learning confidence for out-of-distribution detection in neural networks. *arXiv preprint arXiv:1802.04865*, 2018.

Michael Dusenberry, Ghassen Jerfel, Yeming Wen, Yian Ma, Jasper Snoek, Katherine Heller, Balaji Lakshminarayanan, and Dustin Tran. Efficient and scalable bayesian neural nets with rank-1 factors. In *International conference on machine learning*, pages 2782–2792. PMLR, 2020.

Andre Esteva, Brett Kuprel, Roberto A Novoa, Justin Ko, Susan M Swetter, Helen M Blau, and Sebastian Thrun. Dermatologist-level classification of skin cancer with deep neural networks. *nature*, 542(7639):115–118, 2017.

Angelos Filos, Sebastian Farquhar, Aidan N Gomez, Tim GJ Rudner, Zachary Kenton, Lewis Smith, Milad Alizadeh, Arnoud de Kroon, and Yarin Gal. A systematic comparison of bayesian deep learning robustness in diabetic retinopathy tasks. *arXiv preprint arXiv:1912.10481*, 2019.

Yarin Gal. *Uncertainty in Deep Learning*. PhD thesis, University of Cambridge, 2016.

Yarin Gal and Zoubin Ghahramani. Dropout as a bayesian approximation: Representing model uncertainty in deep learning. In *international conference on machine learning*, pages 1050–1059, 2016.

Yarin Gal, Riashat Islam, and Zoubin Ghahramani. Deep bayesian active learning with image data. In *International Conference on Machine Learning*, pages 1183–1192. PMLR, 2017.

Tilmann Gneiting and Adrian E Raftery. Strictly proper scoring rules, prediction, and estimation. *Journal of the American statistical Association*, 102(477):359–378, 2007.

Henry Gouk, Eibe Frank, Bernhard Pfahringer, and Michael J Cree. Regularisation of neural networks by enforcing lipschitz continuity. *Machine Learning*, 110(2):393–416, 2021.

Ishaan Gulrajani, Faruk Ahmed, Martin Arjovsky, Vincent Dumoulin, and Aaron C Courville. Improved training of wasserstein gans. In *NeurIPS*, 2017.

Chuan Guo, Geoff Pleiss, Yu Sun, and Kilian Q Weinberger. On calibration of modern neural networks. *arXiv preprint arXiv:1706.04599*, 2017.

Kaiming He, Xiangyu Zhang, Shaoqing Ren, and Jian Sun. Deep residual learning for image recognition. In *Proceedings of the IEEE conference on computer vision and pattern recognition*, pages 770–778, 2016.

Dan Hendrycks and Kevin Gimpel. A baseline for detecting misclassified and out-of-distribution examples in neural networks. *arXiv preprint arXiv:1610.02136*, 2016.

Dan Hendrycks, Mantas Mazeika, and Thomas Dietterich. Deep anomaly detection with outlier exposure. In *International Conference on Learning Representations*, 2018.

José Miguel Hernández-Lobato and Ryan Adams. Probabilistic backpropagation for scalable learning of bayesian neural networks. In *International Conference on Machine Learning*, pages 1861–1869. PMLR, 2015.

Sibylle Hess, Wouter Duivesteijn, and Decebal Mocanu. Softmax-based classification is k-means clustering: Formal proof, consequences for adversarial attacks, and improvement through centroid based tailoring. *arXiv preprint arXiv:2001.01987*, 2020.

Geoffrey E Hinton and Drew Van Camp. Keeping the neural networks simple by minimizing the description length of the weights. In *Proceedings of the sixth annual conference on Computational learning theory*, pages 5–13, 1993.

Yu Huang and Yue Chen. Autonomous driving with deep learning: A survey of state-of-art technologies. *arXiv preprint arXiv:2006.06091*, 2020.

Alex Kendall and Yarin Gal. What uncertainties do we need in bayesian deep learning for computer vision? In *Advances in neural information processing systems*, pages 5574–5584, 2017.

Diederik P Kingma and Jimmy Ba. Adam: A method for stochastic optimization. In *ICLR*, 2015.

Diederik P Kingma and Max Welling. Auto-encoding variational bayes. In *ICLR*, 2014.

Alex Krizhevsky, Geoffrey Hinton, et al. Learning multiple layers of features from tiny images. 2009.

Balaji Lakshminarayanan, Alexander Pritzel, and Charles Blundell. Simple and scalable predictive uncertainty estimation using deep ensembles. In *Advances in neural information processing systems*, pages 6402–6413, 2017.

Yann LeCun, Léon Bottou, Yoshua Bengio, and Patrick Haffner. Gradient-based learning applied to document recognition. *Proceedings of the IEEE*, 86(11):2278–2324, 1998.

Kimin Lee, Honglak Lee, Kibok Lee, and Jinwoo Shin. Training confidence-calibrated classifiers for detecting out-of-distribution samples. In *International Conference on Learning Representations*, 2018a.

Kimin Lee, Kibok Lee, Honglak Lee, and Jinwoo Shin. A simple unified framework for detecting out-of-distribution samples and adversarial attacks. In *NeurIPS*, 2018b.

Shiyu Liang, Yixuan Li, and R Srikant. Enhancing the reliability of out-of-distribution image detection in neural networks. In *International Conference on Learning Representations*, 2018.

Jeremiah Zhe Liu, Zi Lin, Shreyas Padhy, Dustin Tran, Tania Bedrax-Weiss, and Balaji Lakshminarayanan. Simple and principled uncertainty estimation with deterministic deep learning via distance awareness. In *NeurIPS*, 2020a.

Weitang Liu, Xiaoyun Wang, John Owens, and Yixuan Li. Energy-based out-of-distribution detection. *Advances in Neural Information Processing Systems*, 33, 2020b.

David JC MacKay. *Bayesian methods for adaptive models*. PhD thesis, California Institute of Technology, 1992.

Takeru Miyato, Toshiki Kataoka, Masanori Koyama, and Yuichi Yoshida. Spectral normalization for generative adversarial networks. In *International Conference on Learning Representations*, 2018.

Kevin P Murphy. *Machine learning: a probabilistic perspective*. MIT press, 2012.

Eric Nalisnick, Akihiro Matsukawa, Yee Whye Teh, Dilan Gorur, and Balaji Lakshminarayanan. Hybrid models with deep and invertible features. In *International Conference on Machine Learning*, pages 4723–4732. PMLR, 2019.

Radford M Neal. *Bayesian learning for neural networks*, volume 118. Springer Science & Business Media, 2012.

Yuval Netzer, Tao Wang, Adam Coates, Alessandro Bissacco, Bo Wu, and Andrew Y Ng. Reading digits in natural images with unsupervised feature learning. 2011.

Yaniv Ovadia, Emily Fertig, Jie Ren, Zachary Nado, David Sculley, Sebastian Nowozin, Joshua Dillon, Balaji Lakshminarayanan, and Jasper Snoek. Can you trust your model’s uncertainty? evaluating predictive uncertainty under dataset shift. In *Advances in Neural Information Processing Systems*, pages 13991–14002, 2019.

Janis Postels, Hermann Blum, Cesar Cadena, Roland Siegwart, Luc Van Gool, and Federico Tombari. Quantifying aleatoric and epistemic uncertainty using density estimation in latent space. *arXiv preprint arXiv:2012.03082*, 2020.

Mihaela Rosca, Theophane Weber, Arthur Gretton, and Shakir Mohamed. A case for new neural network smoothness constraints. *arXiv preprint arXiv:2012.07969*, 2020.

Karen Simonyan and Andrew Zisserman. Very deep convolutional networks for large-scale image recognition. In *International Conference on Learning Representations*, 2015.

Lewis Smith and Yarin Gal. Understanding Measures of Uncertainty for Adversarial Example Detection. In *UAI*, 2018.

Joost van Amersfoort, Lewis Smith, Yee Whye Teh, and Yarin Gal. Uncertainty estimation using a single deep deterministic neural network. In *International Conference on Machine Learning*, pages 9690–9700. PMLR, 2020.

Yeming Wen, Dustin Tran, and Jimmy Ba. Batchensemble: an alternative approach to efficient ensemble and lifelong learning. In *International Conference on Learning Representations*, 2019.

Andrew Gordon Wilson and Pavel Izmailov. Bayesian deep learning and a probabilistic perspective of generalization. *arXiv preprint arXiv:2002.08791*, 2020.

Jim Winkens, Rudy Bunel, Abhijit Guha Roy, Robert Stanforth, Vivek Natarajan, Joseph R Ledsam, Patricia MacWilliams, Pushmeet Kohli, Alan Karthikesalingam, Simon Kohl, et al. Contrastive training for improved out-of-distribution detection. *arXiv preprint arXiv:2007.05566*, 2020.

Han Xiao, Kashif Rasul, and Roland Vollgraf. Fashion-mnist: a novel image dataset for benchmarking machine learning algorithms. *arXiv preprint arXiv:1708.07747*, 2017.

Sergey Zagoruyko and Nikos Komodakis. Wide residual networks. *arXiv preprint arXiv:1605.07146*, 2016.

A AMBIGUOUS- AND DIRTY-MNIST

Each sample in Ambiguous-MNIST is constructed by decoding a linear combination of latent representations of 2 different MNIST digits from a pre-trained VAE [Kingma and Welling, 2014]. Every decoded image is assigned several labels sampled from the softmax probabilities of an off-the-shelf MNIST neural network, with points filtered based on an ensemble’s MI (to remove ‘junk’ images) and then stratified class-wise based on their softmax entropy (some classes are inherently more ambiguous, so we ‘amplify’ these; we stratify per-class to try to preserve a wide spread of possible entropy values, and avoid introducing additional ambiguity which will increase all points to have highest entropy). All off-the-shelf MNIST neural network were then discarded and new models were trained to generate Fig 1 (and as can be seen, the ambiguous points we generate indeed have high entropy regardless of the model architecture used). We create 60K such training and 10K test images to construct Ambiguous-MNIST. Finally, the Dirty-MNIST dataset in this experiment, contains MNIST and Ambiguous-MNIST samples in a 1:1 ratio (with 120K training and 20K test samples).

B ADDITIONAL ARCHITECTURAL CHANGES

Increasing sensitivity: Using residual connections to enforce sensitivity works well in practice when the layer is defined as $x' = x + f(x)$. However, there are several places in the network where additional spatial downsampling is done in $f(\cdot)$ (through a strided convolution), and in order to compute the residual operation x needs to be downsampled as well. These downsampling operations are crucial for managing memory consumption and generalisation. The way this is traditionally done in ResNets is by introducing an additional function $g(\cdot)$ on the residual branch (obtaining $x' = g(x) + f(x)$) which is a strided 1x1 convolution. In practice, the stride is set to 2 pixels, which leads to the output of $g(\cdot)$ only being dependent on the top left pixel of each 2x2 patch, which reduces sensitivity. We overcome this issue by making an architectural change that improves uncertainty quality without sacrificing accuracy. We use a strided average pooling operation instead of a 1x1 convolution in $g(\cdot)$. This makes the output of $g(\cdot)$ dependent on all input pixels. Additionally, we use leaky ReLU activation functions, which are equivalent to ReLU activations when the input is larger than 0, but below 0 they compute $p * x$ with $p = 0.01$ in practice. These further improve sensitivity as all negative activations still propagate in the network.

C EXPERIMENTAL DETAILS

C.1 DIRTY-MNIST

We train for 50 epochs using SGD with a momentum of 0.9 and an initial learning rate of 0.1. The learning rate drops by a factor of 10 at training epochs 25 and 40. Following SNGP [Liu et al., 2020a], we apply online spectral normalisation with one step of power iteration on the convolutional weights. For 1x1 convolutions we use the exact algorithm, and for 3x3 the approximate algorithm from Gouk et al. [2021]. The coefficient for SN is a hyper-parameter which we set to 3 using cross-validation.

C.2 CIFAR-10 VS SVHN/CIFAR-100

We use Wide-ResNet-28-10 [Zagoruyko and Komodakis, 2016] as the model architecture for all the baselines. We train the softmax baselines for 350 epochs using SGD as the optimiser with a momentum of 0.9, and an initial learning rate of 0.1. The learning rate drops by a factor of 10 at epochs 150 and 250. We train the 5-Ensemble baseline using this same training setup. The SNGP and DUQ models were trained using the setup of SNGP and hyper-parameters mentioned in their respective papers [Liu et al., 2020a, van Amersfoort et al., 2020].

D ADDITIONAL EXPERIMENTAL RESULTS (CIFAR-10 VS SVHN/CIFAR-100)

In this section, we provide details of additional results on the OoD detection task using CIFAR-10 vs SVHN/CIFAR-100 for various ablations on DDU. As mentioned in section 4, DDU consists of a deterministic softmax model trained with appropriate inductive biases. It uses softmax entropy to quantify aleatoric uncertainty and feature-space density to quantify epistemic uncertainty. In the ablations, we try to experimentally evaluate the following scenarios:

1. **Effect of inductive biases (sensitivity + smoothness):** We want to see the effect of removing the proposed inductive biases (i.e., no sensitivity and smoothness constraints) on the OoD detection performance of a model. To do this, we train a VGG-16 without spectral normalisation. Note that VGG-16 does not have residual connections and hence, a VGG-16 trained without spectral normalisation does not follow the sensitivity and smoothness (bi-Lipschitz) constraints.
2. **Effect of sensitivity alone:** Since residual connections make a model sensitive to changes in the input space by lower bounding its Lipschitz constant, we also want to see how a network performs with just the sensitivity constraint alone. To observe this, we train a Wide-ResNet-

| Ablations | | | | Aleatoric Uncertainty | Epistemic Uncertainty | Test Accuracy | Test ECE | AUROC SVHN | AUROC CIFAR-100 |
|-------------------|----------------------|----|-----|---------------------------------------|------------------------------------|-------------------------------------|---|-------------------------------------|-------------------------------------|
| Architecture | Residual Connections | SN | GMM | | | | | | |
| Wide-ResNet-28-10 | ✓ | ✗ | ✗ | Softmax Entropy | Softmax Entropy Softmax Density | 96.18 ± 0.07 96.18 ± 0.07 | 0.0073 ± 0.0007 0.0073 ± 0.0007 | 92.99 ± 1.8 92.79 ± 2.03 | 88.08 ± 0.02 87.7 ± 0.02 |
| | | ✓ | ✓ | GMM Entropy Softmax Entropy | GMM Density | 96.09 ± 0.07 96.18 ± 0.07 | 0.0391 ± 0.0007 0.0073 ± 0.0007 | 97.28 ± 0.21 97.28 ± 0.21 | 91.51 ± 0.05 91.51 ± 0.05 |
| | ✓ | ✗ | ✗ | Softmax Entropy | Softmax Entropy Softmax Density | 96.38 ± 0.04 96.38 ± 0.04 | 0.0073 ± 0.0004 | 95.37 ± 0.47 95.59 ± 0.5 | 89.22 ± 0.2 90.17 ± 1.38 |
| | | ✓ | ✓ | GMM Entropy Softmax Entropy | GMM Density | 96.29 ± 0.05 96.38 ± 0.04 | 0.0371 ± 0.0005 0.0073 ± 0.0004 | 97.9 ± 0.22 97.9 ± 0.22 | 91.77 ± 0.05 91.77 ± 0.05 |
| VGG-16 | ✗ | ✗ | ✗ | Softmax Entropy | Softmax Entropy Softmax Density | 94.1 ± 0.05 94.1 ± 0.05 | 0.0174 ± 0.0012 0.0174 ± 0.0012 | 86.88 ± 1.14 86.05 ± 1.22 | 81.72 ± 0.27 81.38 ± 0.31 |
| | | | ✓ | GMM Entropy Softmax Entropy | GMM Density | 93.46 ± 0.24 94.1 ± 0.05 | 0.0654 ± 0.0024 0.0174 ± 0.0012 | 88.56 ± 0.88 88.56 ± 0.88 | 86.7 ± 0.18 86.7 ± 0.18 |

Table 3: *OoD detection performance of different ablations trained on CIFAR-10 using Wide-ResNet-28-10 and VGG-16 architectures with SVHN and CIFAR-100 as OoD datasets.* Note: SN stands for Spectral Normalisation.

28-10 without spectral normalisation (i.e., no explicit upper bound on the Lipschitz constant of the model).

3. Metrics for aleatoric and epistemic uncertainty: With the above combinations, we try to observe how different metrics for aleatoric and epistemic uncertainty perform. To quantify aleatoric uncertainty, we use **i**) the softmax entropy and **ii**) the GMM entropy of a model. Note that the GMM outputs a vector of feature densities, one per class. The GMM entropy is computed by normalising this vector of class-wise feature densities using a softmax function and then computing its entropy. On the other hand, to quantify the epistemic uncertainty, we use **i**) the softmax entropy, **ii**) the softmax density [Liu et al., 2020b] or **iii**) the GMM feature density (as described in section 4).

We present the results of the above ablations in table 3, and can make the following observations (in addition to the ones we make in section 6.3):

Inductive biases are important for feature density. From the AUROC scores in table 3, we can see that using the feature density of a GMM in VGG-16 without the proposed inductive biases yields significantly lower AUROC scores as compared to Wide-ResNet-28-10 with inductive biases. This shows that the GMM feature density alone cannot estimate epistemic uncertainty in a model that suffers from feature collapse. We need sensitivity and smoothness conditions (see section 3) on the feature space of the model to obtain feature densities that capture epistemic uncertainty.

Sensitivity creates a bigger difference than smoothness. We note that the difference between AUROC obtained from feature density between Wide-ResNet-28-10 models with and without spectral normalisation is minimal. Although Wide-ResNet-28-10 with spectral normalisation (i.e., smoothness constraints) still outperforms its counterpart without spectral normalisation, the small difference between the AUROC scores indicates that it might be the residual connections (i.e., sensitivity constraints) that make the model detect OoD samples better. In fact, this observation is also intuitive as a sensitive feature extractor should

map OoD samples far from iD.

GMM Entropy is miscalibrated. We note that the ECE scores of models using a softmax function on the GMM feature densities (GMM Entropy in table 3) are significantly higher than those using a softmax function on network logits (Softmax Entropy/Density in table 3). Well separated features produce sharp Gaussian distributions per class. As a result the softmax outputs from a class-wise GMM feature density vector are always quite confident even when they are inaccurate on iD test samples. Hence, they are miscalibrated and have relatively higher ECE scores.

DDU, the best of both worlds. In DDU we use the softmax output of a model to get aleatoric uncertainty. We use the GMM feature-density to estimate the epistemic uncertainty. Hence, using DDU, we don't suffer from miscalibration as the softmax outputs can be calibrated using post-hoc methods like temperature scaling. At the same time, the feature-densities of the model don't get affected by temperature scaling and capture epistemic uncertainty well.

E 5-ENSEMBLE VISUALISATION

In fig. 4, we provide a visualisation of a 5-ensemble (with five deterministic softmax networks) to see how softmax entropy fails to capture epistemic uncertainty precisely because the mutual information (MI) of an ensemble does not (see section 3). We train the networks on 1 dimensional data with binary labels 0 and 1. The data is shown in fig. 4(b). From fig. 4(a) and fig. 4(b), we find that softmax entropy is high in regions of ambiguity where the label changes from 0 to 1 (i.e., at x value -4 and 4). This indicates that softmax entropy can capture aleatoric uncertainty. Furthermore, in the x interval $(-2, 2)$, we find that the deterministic softmax networks disagree in their predictions (see fig. 4(a)) and have softmax entropies which can be high, low or anywhere in between (see fig. 4(b)) following our claim in section 3. In fact, this disagreement is the very reason why the MI of the ensemble is high in the interval $(-2, 2)$, thereby reliably capturing epistemic uncertainty. Finally, note that the

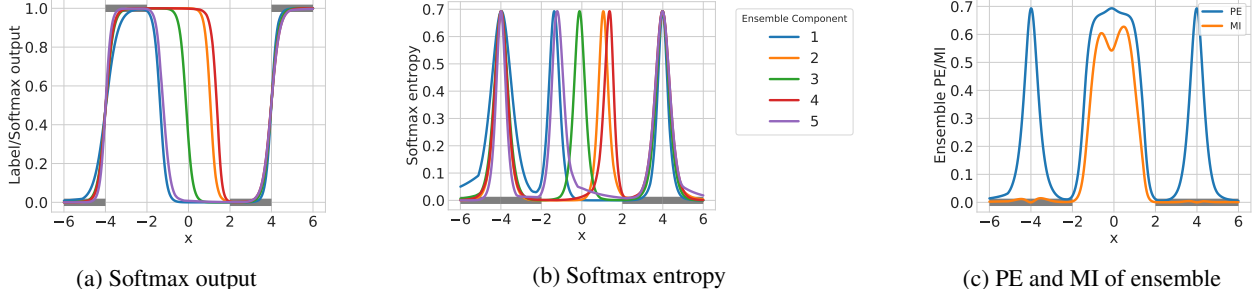


Figure 4: Visualisation of softmax outputs/entropies along with the Predictive Entropy (PE) and Mutual Information of a 5-Ensemble. Figures (a) and (b) show that the softmax entropy is high at points of ambiguity, i.e., where the label changes from 0 to 1 for the data, thereby capturing aleatoric uncertainty, whereas softmax entropy can be low or high for OoD (between -2 to 2). At the same time, figure (c) shows the the MI of the ensemble is only high for OoD, thereby solely capturing epistemic uncertainty, whereas the PE of the ensemble is high for both OoD and for regions of ambiguity, thereby capturing both epistemic and aleatoric uncertainty.

predictive entropy (PE) of the ensemble is high both in the OoD interval $(-2, 2)$ as well as at points of ambiguity (i.e., at -4 and 4). This indicates that the PE of a deep ensemble captures both epistemic and aleatoric uncertainty well. From these visualisations we draw the conclusion that the softmax entropy of a deterministic softmax model cannot capture epistemic uncertainty precisely because the MI of a deep ensemble can.

F THEORETICAL RESULTS

F.1 SOFTMAX ENTROPY CANNOT CAPTURE EPISTEMIC UNCERTAINTY BECAUSE DEEP ENSEMBLES CAN

F.1.1 Qualitative Statement

We start with a proof of proposition 3.1, which shows that given the same predictive entropy, higher epistemic uncertainty will cause some ensemble members to have lower softmax entropy.

The proof requires a lemma:

Lemma F.1 (Law of the Excluded Middle). *Let $(\Omega, \mathcal{A}, \mathbf{P})$ be a probability space and let X be an integrable random variable with expectation $\mathbb{E}[X] = 0$. Then $P[X \geq 0] > 0$ and $P[X \leq 0] > 0$.*

Proof. Assume $P[X = 0] = 0$. Then we have $P[X < 0] + P[X > 0] = 1$, and hence $P[X > 0] > 0$ or $P[X < 0] > 0$. With

$$0 = \mathbb{E}[X|X < 0]P[X < 0] + \mathbb{E}[X|X > 0]P[X > 0], \quad (3)$$

we see that both $P[X > 0], P[X < 0] > 0$. \square

Corollary F.1.1. *Let $(\Omega, \mathcal{A}, \mathbf{P})$ be a probability space and let X be an integrable random variable with expectation $\mathbb{E}[X] = \mu$. Then $P[X \geq \mu] > 0$ and $P[X \leq \mu] > 0$.*

With this, we can prove proposition 3.1:

Proposition 3.1. *Let x_1 and x_2 be points such that x_1 has higher epistemic uncertainty than x_2 under the ensemble: $\mathbb{I}[Y_1; \omega | x_1, \mathcal{D}] > \mathbb{I}[Y_2; \omega | x_2, \mathcal{D}]$. Further assume both have equal predictive entropies $\mathbb{H}[Y_1 | x_1, \mathcal{D}] = \mathbb{H}[Y_2 | x_2, \mathcal{D}]$. Then, there exist sets of ensemble members Ω_1, Ω_2 with $p(\Omega_1 | \mathcal{D}) > 0$ and $p(\Omega_2 | \mathcal{D}) > 0$, such that for all $\omega_1 \in \Omega_1$ and $\omega_2 \in \Omega_2$ the softmax entropy of x_1 is lower than the softmax entropy of x_2 : $\mathbb{H}[Y_1 | x_1, \omega_1] < \mathbb{H}[Y_2 | x_2, \omega_2]$.*

Proof. From eq. (1), we obtain

$$\begin{aligned} & \mathbb{I}[Y_1; \omega | x_1, \mathcal{D}] + \mathbb{E}_{p(\omega | \mathcal{D})} [\mathbb{H}[Y_1 | x_1, \omega]] \\ &= \mathbb{I}[Y_2; \omega | x_2, \mathcal{D}] + \mathbb{E}_{p(\omega | \mathcal{D})} [\mathbb{H}[Y_2 | x_2, \omega]], \end{aligned} \quad (4)$$

and hence

$$\mathbb{E}_{p(\omega | \mathcal{D})} [\mathbb{H}[Y_1 | x_1, \omega]] < \mathbb{E}_{p(\omega | \mathcal{D})} [\mathbb{H}[Y_2 | x_2, \omega]]. \quad (5)$$

Applying lemma F.1, we have

$$P[\mathbb{H}[Y_1 | x_1, \omega, \mathcal{D}] < \mathbb{E}_{p(\omega | \mathcal{D})} [\mathbb{H}[Y_1 | x_1, \omega]]] > 0, \quad (6)$$

and we simply set

$$\Omega_1 = \{\omega : \mathbb{H}[Y_1 | x_1, \omega] < \mathbb{E}_{p(\omega | \mathcal{D})} [\mathbb{H}[Y_1 | x_1, \omega]]\}. \quad (7)$$

Likewise for Ω_2 , and the statement follows. \square

While this statement provides us with an intuition for why ensemble members and thus deterministic models cannot provide epistemic uncertainty reliably through their softmax entropies, we can examine this further by establishing some upper bounds.

F.1.2 Infinite Deep Ensemble

There are two interpretations of the ensemble parameter distribution $p(\omega | \mathcal{D})$: we can view it as an empirical distribution given a specific trained ensemble with members $\omega_{i=1..K}$, or we can view it as a distribution over all possible trained models, given random weight initializations,

the dataset, stochasticity in the minibatches and the optimization process. In that case, any Deep Ensemble with K members can be seen as finite Monte-Carlo sample of this posterior distribution. The predictions of an ensemble then are an unbiased estimate of the predictive distribution $\mathbb{E}_{p(\omega|\mathcal{D})}[p(y|x, \omega)]$, and similarly the information gain computed using the members of the Deep Ensemble is just a (biased) estimator of the true information gain $\mathbb{I}[Y; \omega|x, \mathcal{D}]$.

F.1.3 Analysis of Softmax Entropy of a Single Deterministic Model on OoD Data using Properties of Deep Ensembles

Based on the interpretation of deep ensembles as a distribution over model parameters, we can walk backwards and, given *some value* for the predictive distribution and epistemic uncertainty of a deep ensemble, estimate what the softmax entropies from each ensemble component must have been. I.e. if we observe deep ensembles to have high epistemic uncertainty on OoD data, we can deduce from that what the softmax entropy of deterministic neural nets (the ensemble components) must look like. More specifically, given a predictive distribution $p(y|x)$ and epistemic uncertainty, that is information gain $\mathbb{I}[Y; \omega]$, of the infinite deep ensemble, we estimate the expected mean and variance of the softmax entropies from a single deterministic model, considered as a sample $\omega \sim p(\omega|\mathcal{D})$.

We will need to make several strong assumptions that limit the generality of our estimation, but we can show that our analysis models the resulting softmax entropy distributions appropriately. This will show that deterministic softmax models can have widely different entropies and confidence values.

Given the predictive distribution $p(y|x)$ and epistemic uncertainty $\mathbb{I}[Y; \omega]$ for a single x , we can approximate the distribution over softmax probability vectors $p(y|x, \omega)$ for different ω using its maximum-entropy estimate: a Dirichlet distribution $(Y_1, \dots, Y_K) \sim \text{Dir}(\alpha)$ with non-negative concentration parameters $\alpha = (\alpha_1, \dots, \alpha_K)$ and $\alpha_0 := \sum \alpha_i$. Note that the Dirichlet distribution is used *only as an analysis tool*, and at no point do we need to actually fit Dirichlet distributions to our data.

Preliminaries

Before we can establish our main result, we need to look more closely at Dirichlet-Multinomial distributions. Given a Dirichlet distribution $\text{Dir}(\alpha)$ and a random variable $\mathbf{p} \sim \text{Dir}(\alpha)$, we want to quantify the expected entropy $\mathbb{E}_{\mathbf{p} \sim \text{Dir}(\alpha)} \mathbb{H}_{Y \sim \text{Cat}(\mathbf{p})}[Y]$ and its variance $\text{Var}_{\mathbf{p} \sim \text{Dir}(\alpha)} \mathbb{H}_{Y \sim \text{Cat}(\mathbf{p})}[Y]$. For this, we need to develop more theory. In the following, Γ denotes the Gamma function, ψ denotes the Digamma function, ψ' denotes the Trigamma

function.

Lemma F.2. *Given a Dirichlet distribution and random variable $\mathbf{p} \sim \text{Dir}(\alpha)$, the following hold:*

1. *The expectation $\mathbb{E}[\log \mathbf{p}_i]$ is given by:*

$$\mathbb{E}[\log \mathbf{p}_i] = \psi(\alpha_i) - \psi(\alpha_0). \quad (8)$$

2. *The covariance $\text{Cov}[\log \mathbf{p}_i, \log \mathbf{p}_j]$ is given by*

$$\text{Cov}[\log \mathbf{p}_i, \log \mathbf{p}_j] = \psi'(\alpha_i) \delta_{ij} - \psi'(\alpha_0). \quad (9)$$

3. *The expectation $\mathbb{E}[\mathbf{p}_i^n \mathbf{p}_j^m \log \mathbf{p}_i]$ is given by:*

$$\begin{aligned} \mathbb{E}[\mathbf{p}_i^n \mathbf{p}_j^m \log \mathbf{p}_i] \\ = \frac{\alpha_i^{\bar{n}} \alpha_j^{\bar{m}}}{\alpha_0^{\bar{n+m}}} (\psi(\alpha_i + n) - \psi(\alpha_0 + n + m)), \end{aligned} \quad (10)$$

where $i \neq j$, and $\bar{n} = n(n+1) \dots (n+k-1)$ denotes the rising factorial.

Proof. 1. The Dirichlet distribution is members of the exponential family. Therefore the moments of the sufficient statistics are given by the derivatives of the partition function with respect to the natural parameters. The natural parameters of the Dirichlet distribution are just its concentration parameters α_i . The partition function is

$$A(\alpha) = \sum_{i=1}^k \log \Gamma(\alpha_i) - \log \Gamma(\alpha_0), \quad (11)$$

the sufficient statistics is $T(x) = \log x$, and the expectation $\mathbb{E}[T]$ is given by

$$\mathbb{E}[T_i] = \frac{\partial A(\alpha)}{\partial \alpha_i} \quad (12)$$

as the Dirichlet distribution is a member of the exponential family. Substituting the definitions and evaluating the partial derivative yields

$$\mathbb{E}[\log \mathbf{p}_i] = \frac{\partial}{\partial \alpha_i} \left[\sum_{i=1}^k \log \Gamma(\alpha_i) - \log \Gamma\left(\sum_{i=1}^k \alpha_i\right) \right] \quad (13)$$

$$= \psi(\alpha_i) - \psi(\alpha_0) \frac{\partial}{\partial \alpha_i} \alpha_0, \quad (14)$$

where we have used that the Digamma function ψ is the log derivative of the Gamma function $\psi(x) = \frac{d}{dx} \ln \Gamma(x)$. This proves (8) as $\frac{\partial}{\partial \alpha_i} \alpha_0 = 1$.

2. Similarly, the covariance is obtained using a second-order partial derivative:

$$\text{Cov}[T_i, T_j] = \frac{\partial^2 A(\alpha)}{\partial \alpha_i \partial \alpha_j}. \quad (15)$$

Again, substituting yields

$$\text{Cov}[\log \mathbf{p}_i, \log \mathbf{p}_j] = \frac{\partial}{\partial \alpha_j} [\psi(\alpha_i) - \psi(\alpha_0)] \quad (16)$$

$$= \psi'(\alpha_i) \delta_{ij} - \psi'(\alpha_0). \quad (17)$$

3. We will make use of a simple reparameterization to prove the statement using eq. (8). Expanding the expectation and substituting the density $\text{Dir}(\mathbf{p}; \alpha)$, we obtain

$$\mathbb{E} [\mathbf{p}_i^n \mathbf{p}_j^m \log \mathbf{p}_i] = \int \text{Dir}(\mathbf{p}; \alpha) \mathbf{p}_i^n \mathbf{p}_j^m \log \mathbf{p}_i d\mathbf{p} \quad (18)$$

$$= \int \frac{\Gamma(\alpha_0)}{\prod_{i=1}^K \Gamma(\alpha_i)} \prod_{k=1}^K \mathbf{p}_k^{\alpha_k-1} \mathbf{p}_i^n \mathbf{p}_j^m \log \mathbf{p}_i d\mathbf{p} \quad (19)$$

$$= \frac{\Gamma(\alpha_i+n)\Gamma(\alpha_j+m)\Gamma(\alpha_0+n+m)}{\Gamma(\alpha_i)\Gamma(\alpha_j)\Gamma(\alpha_0)} \quad (20)$$

$$\begin{aligned} & \int \text{Dir}(\hat{\mathbf{p}}; \hat{\alpha}) \hat{\mathbf{p}}_i^n \hat{\mathbf{p}}_j^m \log \hat{\mathbf{p}}_i d\hat{\mathbf{p}} \\ &= \frac{\alpha_i^{\bar{n}} \alpha_j^{\bar{m}}}{\alpha_0^{n+m}} \mathbb{E} [\log \hat{\mathbf{p}}_i], \end{aligned} \quad (21)$$

where $\hat{\mathbf{p}} \sim \text{Dir}(\hat{\alpha})$ with $\hat{\alpha} = (\alpha_0, \dots, \alpha_i + n, \dots, \alpha_j + m, \dots, \alpha_K)$ and we made use of the fact that $\frac{\Gamma(z+n)}{\Gamma(z)} = z^{\bar{n}}$. Finally, we can apply eq. (8) on $\hat{\mathbf{p}} \sim \text{Dir}(\hat{\alpha})$ to show

$$= \frac{\alpha_i^{\bar{n}} \alpha_j^{\bar{m}}}{\alpha_0^{n+m}} (\psi(\alpha_i+n) - \psi(\alpha_0+n+m)). \quad (22)$$

□

With this, we can already quantify the expected entropy $\mathbb{E}_{\mathbf{p} \sim \text{Dir}(\alpha)} \mathbb{H}_{Y \sim \text{Cat}(\mathbf{p})}[Y]$:

Lemma F.3. *Given a Dirichlet distribution and random variable $\mathbf{p} \sim \text{Dir}(\alpha)$, the expected entropy $\mathbb{E}_{\mathbf{p} \sim \text{Dir}(\alpha)} \mathbb{H}_{Y \sim \text{Cat}(\mathbf{p})}[Y]$ of the categorical distribution $Y \sim \text{Cat}(\mathbf{p})$ is given by*

$$\mathbb{E}_{\mathbf{p}(\mathbf{p}|\alpha)} \mathbb{H}[Y | \mathbf{p}] = \psi(\alpha_0+1) - \sum_{y=1}^K \frac{\alpha_i}{\alpha_0} \psi(\alpha_i+1). \quad (23)$$

Proof. Applying the sum rule of expectations and eq. (10) from Lemma F.2, we can write

$$\mathbb{E} \mathbb{H}[Y | \mathbf{p}] = \mathbb{E} \left[- \sum_{i=1}^K \mathbf{p}_i \log \mathbf{p}_i \right] = - \sum_i \mathbb{E} [\mathbf{p}_i \log \mathbf{p}_i] \quad (24)$$

$$= - \sum_i \frac{\alpha_i}{\alpha_0} (\psi(\alpha_i+1) - \psi(\alpha_0+1)). \quad (25)$$

The result follows after rearranging and making use of $\sum_i \frac{\alpha_i}{\alpha_0} = 1$. □

With these statements, we can answer a slightly more complex problem:

Lemma F.4. *Given a Dirichlet distribution and random variable $\mathbf{p} \sim \text{Dir}(\alpha)$, the covariance*

$\text{Cov}[\mathbf{p}_i^n \log \mathbf{p}_i, \mathbf{p}_j^m \log \mathbf{p}_j]$ is given by

$$\text{Cov}[\mathbf{p}_i^n \log \mathbf{p}_i, \mathbf{p}_j^m \log \mathbf{p}_j] \quad (26)$$

$$\begin{aligned} &= \frac{\alpha_i^{\bar{n}} \alpha_j^{\bar{m}}}{\alpha_0^{n+m}} ((\psi(\alpha_i+n) - \psi(\alpha_0+n+m)) \\ &\quad (\psi(\alpha_j+m) - \psi(\alpha_0+n+m)) \\ &\quad - \psi'(\alpha_0+n+m)) \\ &\quad + \frac{\alpha_i^{\bar{n}} \alpha_j^{\bar{m}}}{\alpha_0^{\bar{n}} \alpha_0^{\bar{m}}} (\psi(\alpha_i+n) - \psi(\alpha_0+n)) \\ &\quad (\psi(\alpha_j+m) - \psi(\alpha_0+n)), \end{aligned} \quad (27)$$

for $i \neq j$, where ψ is the Digamma function and ψ' is the Trigamma function. Similarly, the covariance $\text{Cov}[\mathbf{p}_i^n \log \mathbf{p}_i, \mathbf{p}_i^m \log \mathbf{p}_i]$ is given by

$$\text{Cov}[\mathbf{p}_i^n \log \mathbf{p}_i, \mathbf{p}_i^m \log \mathbf{p}_i] \quad (28)$$

$$\begin{aligned} &= \frac{\alpha_i^{\bar{n+m}}}{\alpha_0^{\bar{n+m}}} ((\psi(\alpha_i+n+m) - \psi(\alpha_0+n+m))^2 \\ &\quad + \psi'(\alpha_i+n+m) - \psi'(\alpha_0+n+m)) \\ &\quad + \frac{\alpha_i^{\bar{n}} \alpha_i^{\bar{m}}}{\alpha_0^{\bar{n}} \alpha_0^{\bar{m}}} (\psi(\alpha_i+n) - \psi(\alpha_0+n)) \\ &\quad (\psi(\alpha_i+m) - \psi(\alpha_0+n)). \end{aligned} \quad (29)$$

Regrettably, the equations are getting large. By abuse of notation, we introduce a convenient shorthand, before proving the proof of the lemma.

Definition F.5. *We will denote by*

$$\overline{\mathbb{E} [\log \hat{\mathbf{p}}_i^{n,m}]} = \psi(\alpha_i+n) - \psi(\alpha_0+n+m), \quad (30)$$

and use $\overline{\mathbb{E} [\log \hat{\mathbf{p}}_i^n]}$ for $\overline{\mathbb{E} [\log \hat{\mathbf{p}}_i^{n,0}]}$. Likewise,

$$\overline{\text{Cov}[\log \hat{\mathbf{p}}_i^{n,m}, \log \hat{\mathbf{p}}_j^{n,m}]} = \psi'(\alpha_i+n) \delta_{ij} - \psi'(\alpha_0+n+m). \quad (31)$$

This notation agrees with the proofs of eq. (8) and (9) in Lemma F.2. With this, we can significantly simplify the previous statements:

Corollary F.5.1. *Given a Dirichlet distribution and random variable $\mathbf{p} \sim \text{Dir}(\alpha)$,*

$$\mathbb{E} [\mathbf{p}_i^n \mathbf{p}_j^m \log \mathbf{p}_i] = \frac{\alpha_i^{\bar{n}} \alpha_j^{\bar{m}}}{\alpha_0^{n+m}} \overline{\mathbb{E} [\log \hat{\mathbf{p}}_i^{n,m}]}, \quad (32)$$

$$\text{Cov}[\mathbf{p}_i^n \log \mathbf{p}_i, \mathbf{p}_j^m \log \mathbf{p}_j] \quad (33)$$

$$= \frac{\alpha_i^{\bar{n}} \alpha_j^{\bar{m}}}{\alpha_0^{\bar{n}+\bar{m}}} \left(\overline{\mathbb{E}[\log \hat{\mathbf{p}}_i^{\bar{n}, \bar{m}}]} \overline{\mathbb{E}[\log \hat{\mathbf{p}}_j^{\bar{m}, \bar{n}}]} \right. \\ \left. \overline{\text{Cov}[\log \hat{\mathbf{p}}_i^{\bar{n}, \bar{m}}, \log \hat{\mathbf{p}}_j^{\bar{n}, \bar{m}}]} \right) \\ + \frac{\alpha_i^{\bar{n}} \alpha_j^{\bar{m}}}{\alpha_0^{\bar{n}} \alpha_0^{\bar{m}}} \overline{\mathbb{E}[\log \hat{\mathbf{p}}_i^{\bar{n}}]} \overline{\mathbb{E}[\log \hat{\mathbf{p}}_j^{\bar{m}}]} \quad \text{for } i \neq j, \text{ and} \quad (34)$$

$$\text{Cov}[\mathbf{p}_i^n \log \mathbf{p}_i, \mathbf{p}_i^m \log \mathbf{p}_i] \quad (35)$$

$$= \frac{\alpha_i^{\bar{n}+\bar{m}}}{\alpha_0^{\bar{n}+\bar{m}}} \left(\overline{\mathbb{E}[\log \hat{\mathbf{p}}_i^{\bar{n}+\bar{m}}]}^2 \right. \\ \left. + \overline{\text{Cov}[\log \hat{\mathbf{p}}_i^{\bar{n}+\bar{m}}, \log \hat{\mathbf{p}}_i^{\bar{n}+\bar{m}}]} \right) \\ + \frac{\alpha_i^{\bar{n}} \alpha_i^{\bar{m}}}{\alpha_0^{\bar{n}} \alpha_0^{\bar{m}}} \overline{\mathbb{E}[\log \hat{\mathbf{p}}_i^{\bar{n}}]} \overline{\mathbb{E}[\log \hat{\mathbf{p}}_j^{\bar{m}}]}. \quad (36)$$

Proof of Lemma F.4. This proof applies the well-known formula (**rcov**) $\text{Cov}[X, Y] = \mathbb{E}[XY] - \mathbb{E}[X]\mathbb{E}[Y]$ once forward and once backward (**rcov**) $\mathbb{E}[XY] = \text{Cov}[X, Y] + \mathbb{E}[X]\mathbb{E}[Y]$ while applying eq. (10) several times:

$$\text{Cov}[\mathbf{p}_i^n \log \mathbf{p}_i, \mathbf{p}_j^m \log \mathbf{p}_j] \quad (37)$$

$$\stackrel{\text{cov}}{=} \mathbb{E}[\mathbf{p}_i^n \log(\mathbf{p}_i) \mathbf{p}_j^m \log(\mathbf{p}_j)] \\ - \mathbb{E}[\mathbf{p}_i^n \log \mathbf{p}_i] \mathbb{E}[\mathbf{p}_j^m \log \mathbf{p}_j] \quad (38)$$

$$= \frac{\alpha_i^{\bar{n}} \alpha_j^{\bar{m}}}{\alpha_0^{\bar{n}+\bar{m}}} \mathbb{E}[\log(\hat{\mathbf{p}}_i^{i,j}) \log(\hat{\mathbf{p}}_j^{i,j})] \\ - \mathbb{E}[\log \hat{\mathbf{p}}_i^i] \mathbb{E}[\log \mathbf{p}_j^j] \quad (39)$$

$$\stackrel{(\text{rcov})}{=} \frac{\alpha_i^{\bar{n}} \alpha_j^{\bar{m}}}{\alpha_0^{\bar{n}+\bar{m}}} \left(\text{Cov}[\log \hat{\mathbf{p}}_i^{i,j}, \log \hat{\mathbf{p}}_j^{i,j}] \right. \\ \left. + \mathbb{E}[\log \hat{\mathbf{p}}_i^{i,j}] \mathbb{E}[\log \hat{\mathbf{p}}_j^{i,j}] \right) \quad (40) \\ - \frac{\alpha_i^{\bar{n}} \alpha_j^{\bar{m}}}{\alpha_0^{\bar{n}} \alpha_0^{\bar{m}}} \mathbb{E}[\log \hat{\mathbf{p}}_i^i] \mathbb{E}[\log \mathbf{p}_j^j],$$

where $\mathbf{p}^{i,j} \sim \text{Dir}(\alpha^{i,j})$ with $\alpha^{i,j} = (\dots, \alpha_i + n, \dots, \alpha_j + m, \dots)$. $\mathbf{p}^{i,j}$ and $\alpha^{i,j}$ are defined analogously. Applying eq. (9) and eq. (8) from Lemma F.2 yields the statement. For $i = j$, the proof follows the same pattern. \square

Now, we can prove the theorem that quantifies the variance of the entropy of Y :

Theorem F.6. *Given a Dirichlet distribution and random variable $\mathbf{p} \sim \text{Dir}(\alpha)$, the variance of the entropy $\text{Var}_{\mathbf{p} \sim \text{Dir}(\alpha)} \mathbb{H}_{Y \sim \text{Cat}(\mathbf{p})}[Y]$ of the categorical distribution $Y \sim$*

$\text{Cat}(\mathbf{p})$ is given by

$$\text{Var}[\mathbb{H}[Y | \mathbf{p}]] \quad (41)$$

$$= \sum_i \frac{\alpha_i^{\bar{2}}}{\alpha_0^{\bar{2}}} \left(\overline{\text{Cov}[\log \hat{\mathbf{p}}_i^2, \log \hat{\mathbf{p}}_i^2]} + \overline{\mathbb{E}[\log \hat{\mathbf{p}}_i^2]}^2 \right) \\ + \sum_{i \neq j} \frac{\alpha_i \alpha_j}{\alpha_0^{\bar{2}}} \left(\overline{\text{Cov}[\log \hat{\mathbf{p}}_i^1, \log \hat{\mathbf{p}}_j^1]} + \overline{\mathbb{E}[\log \hat{\mathbf{p}}_i^{1,1}]} \overline{\mathbb{E}[\log \hat{\mathbf{p}}_j^{1,1}]} \right) \\ - \sum_{i,j} \frac{\alpha_i \alpha_j}{\alpha_0^{\bar{2}}} \overline{\mathbb{E}[\log \hat{\mathbf{p}}_i^1]} \overline{\mathbb{E}[\log \hat{\mathbf{p}}_j^1]}. \quad (42)$$

Proof. We start by applying the well-known formula $\text{Var}[\sum_i X_i] = \sum_{i,j} \text{Cov}[X_i, X_j]$ and then apply Lemma F.4 repeatedly. \square

Main Result

All of the above allows us to formulate our main result for some ensemble with a given predictive $\mathbf{p}(y|x)$ and MI $\mathbb{I}[Y; \omega]$:

Theorem F.7. *Fix $\mathbf{p}(y|x)$, $\mathbb{I}[Y; \omega]$, a distribution over models $\mathbf{p}(\omega | \mathcal{D})$, and a sample x . The maximum-entropy estimate of the distribution over probability vectors $\mathbf{p}(y|x, \omega)$ for models $\omega \sim \mathbf{p}(\omega | \mathcal{D})$ given $\mathbf{p}(y|x)$ and $\mathbb{I}[Y; \omega]$ is a Dirichlet distribution $\mathbf{p} \sim \text{Dir}(\alpha)$ that satisfies:*

$$\mathbf{p}(y|x) = \frac{\alpha_i}{\alpha_0} \quad (43)$$

$$\mathbb{H}[Y | x] - \mathbb{I}[Y; \omega] = \psi(\alpha_0 + 1) \\ - \sum_{y=1}^K \mathbf{p}(y|x) \psi(\alpha_0 \mathbf{p}(y|x) + 1). \quad (44)$$

The variance $\text{Var}[\mathbb{H}[Y | x, \omega]]$ of the softmax entropy over models $\omega \sim \mathbf{p}(\omega | \mathcal{D})$ is bounded by $\text{Var}[\mathbb{H}[Y | \mathbf{p}]]$:

$$\text{Var}_{\omega}[\mathbb{H}[Y | x, \omega]] \geq \text{Var}_{\mathbf{p}}[\mathbb{H}[Y | \mathbf{p}]] \quad (45)$$

with the latter term given in eq. (42).

Proof. We can use moment matching to fix the distribution. Equation (43) is just the mean $\mathbb{E}[Y]$, and eq. (44) follows from eq. (1) and Lemma F.3 when we substitute $\frac{\alpha_i}{\alpha_0} = \mathbf{p}_i$. It is easy to check that eq. (44) is monotonously increasing in α_0 , which is thus uniquely determined. Furthermore, we can use the variance of the entropy of the maximum-entropy estimate as a lower-bound because the Dirichlet distribution is a maximum-entropy distribution. \square

Given that we can view an ensemble member as a single deterministic model and vice-versa, this provides an intuitive explanation for why single deterministic models report inconsistent and widely varying predictive entropies and confidence scores for OoD samples for which a Deep Ensemble

would report high epistemic uncertainty (information gain) and high predictive entropy.

Corollary F.7.1. *Assuming that $p(y|x, \omega)$ only depends on $p(y|x)$ and $\mathbb{I}[Y; \omega]$, the maximum-entropy estimate for the distribution $p(y|x, \omega)$ for a given ω and different OoD x is given by a Dirichlet distribution $\text{Dir}(\alpha)$ that satisfies:*

$$p(y|x) = \frac{\alpha_i}{\alpha_0} \quad (46)$$

$$\mathbb{H}[Y|x] - \mathbb{I}[Y; \omega] = \psi(\alpha_0 + 1) \quad (47)$$

$$- \sum_{y=1}^K p(y|x) \psi(\alpha_0 p(y|x) + 1) \dots \quad (48)$$

Then, we can model the softmax distribution using a random variable $\mathbf{p} \sim \text{Dir}(\alpha)$ as:

$$p(y|x, \omega) \stackrel{\sim}{=} \text{Cat}(\mathbf{p}). \quad (49)$$

The variance $\text{Var}[\mathbb{H}[Y|x, \omega]]$ of the softmax entropy for different samples x given $p(y|x)$ and $\mathbb{I}[Y; \omega]$ is bounded by $\text{Var}[\mathbb{H}[Y|\mathbf{p}]]$:

$$\text{Var}_{\omega}[\mathbb{H}[Y|x, \omega]] \geq \text{Var}_{\mathbf{p}}[\mathbb{H}[Y|\mathbf{p}]] \quad (50)$$

with the latter term given in eq. (42).

We empirically find this to be true.

Empirical Results

We empirically verify that softmax entropies vary considerably in fig. 5. In fig. 6, we verify the validity of eq. (45) empirically. Moreover, fig. 6(d) shows both **i**) the non-linear relationship between epistemic uncertainty and variance in the softmax entropies and **ii**) that Dirichlet distributions cannot capture it and can only provide a lower bound. Nonetheless, this simple approximation seems to be able to capture the empirical entropy distribution quite well as shown in fig. 7.

F.2 CAPTURING ALEATORIC AND EPISTEMIC UNCERTAINTY REQUIRES MULTIPLE HIDDEN-LATENT MODELS

In section 3, we noted that the objectives that lead to optimal estimators for aleatoric and epistemic uncertainty via softmax entropy and feature-space density do not match, and DDU therefore uses the softmax layer as a discriminative classifier (implicit LDA) to estimate the predictive entropy, while it is using a GMM as generative classifier to estimate the feature-space density. Here we prove this.

F.2.1 Preliminaries

Before we prove Proposition 3.3, we will introduce some additional notation.

Definition F.8. 1. $\hat{p}(y, z)$ is the data distribution of the \mathcal{D} in feature space with class labels y and feature representation z .

2. $p_{\theta}(\cdot)$ is a probability distribution parameterized by θ .

3. Entropies and conditional entropies are over the empirical data distribution $\hat{p}(\cdot)$:

$$\mathbb{H}[\cdot] = \mathbb{H}(\hat{p}(\cdot)) = \mathbb{E}_{\hat{p}(\cdot)}[-\log \hat{p}(\cdot)]. \quad (51)$$

4. $\mathbb{H}[Y|z]$ is the entropy of $\hat{p}(y|z)$ for a given z , whereas $\mathbb{H}[Y|Z]$ is the conditional entropy:

$$\mathbb{H}[Y|Z] = \mathbb{E}_{\hat{p}(z)} \mathbb{H}[Y|z]. \quad (52)$$

5. $\mathbb{H}(p(y, z) || q(y|z))$ is the cross-entropy of $q(y|z)$ under $p(y|z)$ in expectation over $p(z)$:

$$\begin{aligned} \mathbb{H}(p(y, z) || q(y|z)) &= \mathbb{E}_{p(z)} \mathbb{H}(p(y|z) || q(y|z)) \\ &= \mathbb{E}_{p(y, z)}[-\log q(y|z)]. \end{aligned}$$

6. Similarly, $D_{\text{KL}}(p(y, z) || q(y|z))$ is the Kullback-Leibler divergence of $q(y|z)$ under $p(y|z)$ in expectation over $p(z)$:

$$\begin{aligned} D_{\text{KL}}(p(y, z) || q(y|z)) &= \mathbb{E}_{p(z)} D_{\text{KL}}(p(y|z) || q(y|z)) \\ &= \mathbb{H}(p(y, z) || q(y|z)) - \mathbb{H}[Y|Z] \end{aligned}$$

7. For cross-entropies of $p_{\theta}(\cdot)$ under $\hat{p}(z, y)$, we use the convenient short-hand $\mathbb{H}_{\theta}[\cdot] = \mathbb{H}(\hat{p}(z, y) || p_{\theta}(\cdot))$.

Then we can observe the following connection between $\mathbb{H}_{\theta}[\cdot]$ and $\mathbb{H}[\cdot]$:

Lemma F.9. Cross-entropies upper-bound the respective entropy with equality when $p_{\theta}(\cdot) = \hat{p}(\cdot)$, which is important for variational arguments:

1. $\mathbb{H}_{\theta}[Y, Z] \geq \mathbb{H}[Y, Z]$,
2. $\mathbb{H}_{\theta}[Z] \geq \mathbb{H}[Z]$, and
3. $\mathbb{H}_{\theta}[Y|Z] \geq \mathbb{H}[Y|Z]$.

Proof. 1. $\mathbb{H}_{\theta}[Y, Z] - \mathbb{H}[Y, Z] = D_{\text{KL}}(\hat{p}(y, z) || p_{\theta}(y, z)) \geq 0$.

2. follows from item 1.

3. We expand the expectations and note that inequality commutes with expectations:

$$\mathbb{H}_{\theta}[Y|Z] - \mathbb{H}[Y|Z] = \mathbb{E}_{\hat{p}(z)} [\mathbb{H}_{\theta}[Y|z] - \mathbb{H}[Y|z]] \geq 0,$$

because $\mathbb{H}_{\theta}[Y|z] - \mathbb{H}[Y|z] \geq 0$ for all z . The equality conditions follows from the properties of the Kullback-Leibler divergence as well. \square

We also have:

Lemma F.10.

$$\mathbb{H}_{\theta}[Y, Z] = \mathbb{H}_{\theta}[Y|Z] + \mathbb{H}_{\theta}[Z] \quad (53)$$

$$= \mathbb{H}_{\theta}[Z|Y] + \mathbb{H}_{\theta}[Y]. \quad (54)$$

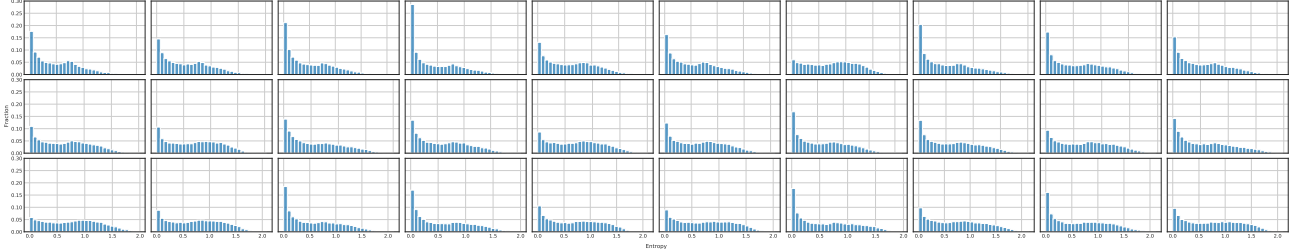


Figure 5: Softmax entropy histograms of 30 Wide-ResNet-28-10+SN models trained on CIFAR-10, evaluated on SVHN (OoD). The softmax entropy distribution of the different models varies considerably.

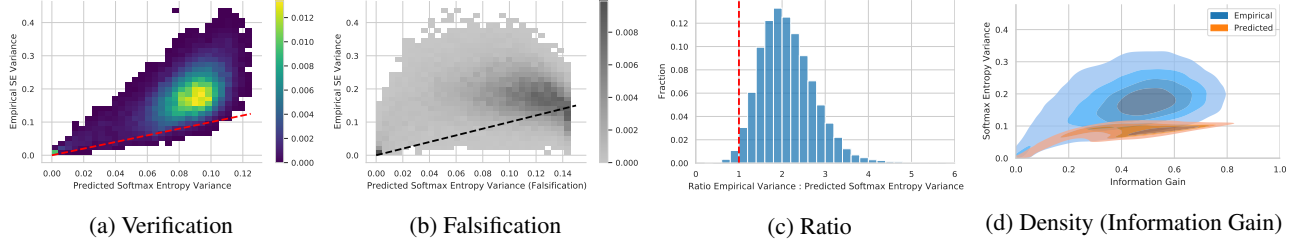


Figure 6: Variance of softmax entropies can be lower-bounded by fitting Dirichlet distributions on the samples $p(y|x, \omega)$. (a) The empirical variance of softmax entropies is lower-bounded by the prediction using theorem F.7. The red dashed line depicts equality. (b) Using uniform predictions in eq. (45) leads to a violation of the predicted lower bounds (black dashed line). (c) The ratio histogram shows that there are only few violations due to precision issues (< 2% (a) vs < 22% for (b), not depicted). (d) The variance of the softmax entropy is not linearly correlated to the epistemic uncertainty. For both high and low epistemic uncertainty, the variance decreases. It is still lower-bounded by eq. (45).

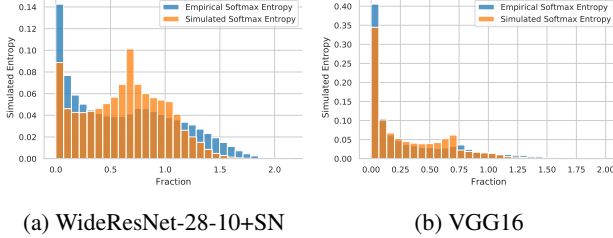


Figure 7: Simulated vs empirical softmax entropy on WideResNet-28-10+SN and VGG16. Even though the Dirichlet variance approximation lower-bounds the empirical softmax entropy variance, sampling from the fitted Dirichlet distributions does approximate the empirical entropy distribution quite well.

Proof. We substitute the definitions and obtain:

$$\mathbb{H}_\theta[Y, Z] = \mathbb{E}_{p(y, z)}[-\log q(y, z)] \quad (55)$$

$$= \mathbb{E}_{p(y, z)}[-\log q(y|z)] + \mathbb{E}_{p(y, z)}[-\log q(z)] \quad (56)$$

$$= \mathbb{H}_\theta[Y|Z] + \mathbb{H}_\theta[Z]. \quad (57)$$

□

The same holds for entropies: $\mathbb{H}[Y, Z] = \mathbb{H}[Y|Z] + \mathbb{H}[Z] = \mathbb{H}[Y|Z] + \mathbb{H}[Y]$ [Cover, 1999].

F.2.2 Proof

We can now prove the observation.

Proposition 3.3. For an input x , let $z = f_\theta(x)$ denote its feature representation in a feature extractor f_θ with parameters θ . Then the following hold:

1. A discriminative classifier $p(y|z)$, e.g. a softmax layer, is well-calibrated in its predictions when it maximises the conditional log-likelihood $\log p(y|z)$;
2. A feature-space density estimator $q(z)$ is optimal when it maximises the marginalised log-likelihood $\log q(z)$;
3. A hidden-latent model $q(y, z)$ cannot generally maximise both objectives, conditional log-likelihood and marginalised log-likelihood, at the same time. In the specific instance that it does maximise both, the resulting model must be a GDA (but the opposite does not hold).

Proof. 1. The conditional log-likelihood is a strictly proper scoring rule [Gneiting and Raftery, 2007]. The optimization objective can be rewritten as

$$\max_\theta \mathbb{E}_{\log p_\theta(y|z)} = \min_\theta \mathbb{H}_\theta[Y|Z] \geq \mathbb{H}[Y|Z]. \quad (58)$$

An optimal discriminative classifier $p_\theta(y|z)$ would thus capture the true (empirical) distribution everywhere: $p_\theta(y|z) = \hat{p}(y|z)$. This means the negative conditional log-likelihood

will be equal $\mathbb{H}[Y|Z]$ and $\mathbb{H}_\theta[Y|z] = \mathbb{H}[Y|z]$ for all z . $\mathbb{H}[Y|z]$ is the irreducible residual conditional entropy, the aleatoric uncertainty.

2. For density estimation $q(z)$, the maximum likelihood $\mathbb{E}[\log q(z)]$ using the empirical data distribution is maximized. We can rewrite this as

$$\max_\theta \mathbb{E}_{\hat{p}(y,z)} \log p_\theta(z) = \min_\theta \mathbb{H}_\theta[Z] \geq \mathbb{H}[Z]. \quad (59)$$

We see that the negative marginalized likelihood of the density estimator upper-bounds the entropy of the feature representations $\mathbb{H}[Z]$. We have equality and $p_\theta(z) = \hat{p}(z)$ in the optimum case.

3. Using $\mathbb{H}_\theta[Y, Z] = \mathbb{H}_\theta[Z|Y] + \mathbb{H}_\theta[Y]$, we can relate the objectives from eq. (58) and (59) to each other. First, we characterize a shared optimum, and then we show that both objectives are generally not minimized at the same time. For both objectives to be minimized, we have $\nabla \mathbb{H}_\theta[Z|Y] = 0$ and $\nabla \mathbb{H}_\theta[Z] = 0$, and we obtain

$$\nabla \mathbb{H}_\theta[Y, Z] = \nabla \mathbb{H}_\theta[Z|Y] + \nabla \mathbb{H}_\theta[Y] = 0. \quad (60)$$

From this we conclude that for minimizing both objectives also minimizes $\mathbb{H}_\theta[Y, Z]$, and that generally the objectives trade-off with each other at stationary points θ of $\mathbb{H}_\theta[Y, Z]$:

$$\nabla \mathbb{H}_\theta[Z|Y] = -\nabla \mathbb{H}_\theta[Y] \quad \text{when } \nabla \mathbb{H}_\theta[Y, Z] = 0 \quad (61)$$

As can easily be verified, a trivial minimizer $q^*(y, z)$ for $\mathbb{H}_\theta[Y, Z]$ given an empirical data distribution $\hat{p}(y, z)$ is an adapted Parzen estimator:

$$q^*(y, z) = \sum_y \hat{p}(y) \mathbb{E}_{\hat{z} \sim \hat{p}(z|y)} \mathcal{N}(z; \hat{z}, \sigma^2 \mathbf{I}), \quad (62)$$

for small enough σ . However, generally, there is no guaranteed shared optimum for other generative classifiers.

Specifically, we will examine GMMs with one component per class. Minimizing $\mathbb{H}_\theta[Y, Z]$ on an empirical data distribution is equivalent to Gaussian Discriminant Analysis, as is easy to check, and minimizing $\mathbb{H}_\theta[Z]$ is equivalent to fitting a density estimator, following eq. (59). The difference is that using a GMM as a density estimator does not constrain the component assignment, unlike in GDA. Consequently, we can intuitively see that *all objectives can be minimized at the same time exactly when the feature representations of different classes are perfectly separated*, such that a GMM fit as density estimator would assign each class's feature representations to a single component.

By the above, we can construct a simple example that shows this: if we have two classes whose features lie in well-separated clusters, GDA will minimize all objectives. The opposite does not hold: it will fail for example if some of the class labels are flipped. An optimal density estimator will still fit to the original clusters, while GDA will not.

Given that perfect separation is impossible with ambiguous data, a shared optimum is rare, but only then is GDA optimal.

In all other cases, GDA does not optimize both objectives, and neither can any other GMM (with one component per class). Moreover, eq. (61) shows that a GMM fit using EM is a better density estimator than GDA, and a softmax layer is a better classifier, as optimizing the softmax objective $\mathbb{H}_\theta[Y|Z]$ or density objective $\mathbb{H}[Z]$ using gradient descent will move away from the GDA optimum.

□